iScience

CellPress
OPEN ACCESS

Article

# Sox17 Promotes Oligodendrocyte Regeneration by Dual Modulation of Hedgehog and Wnt Signaling

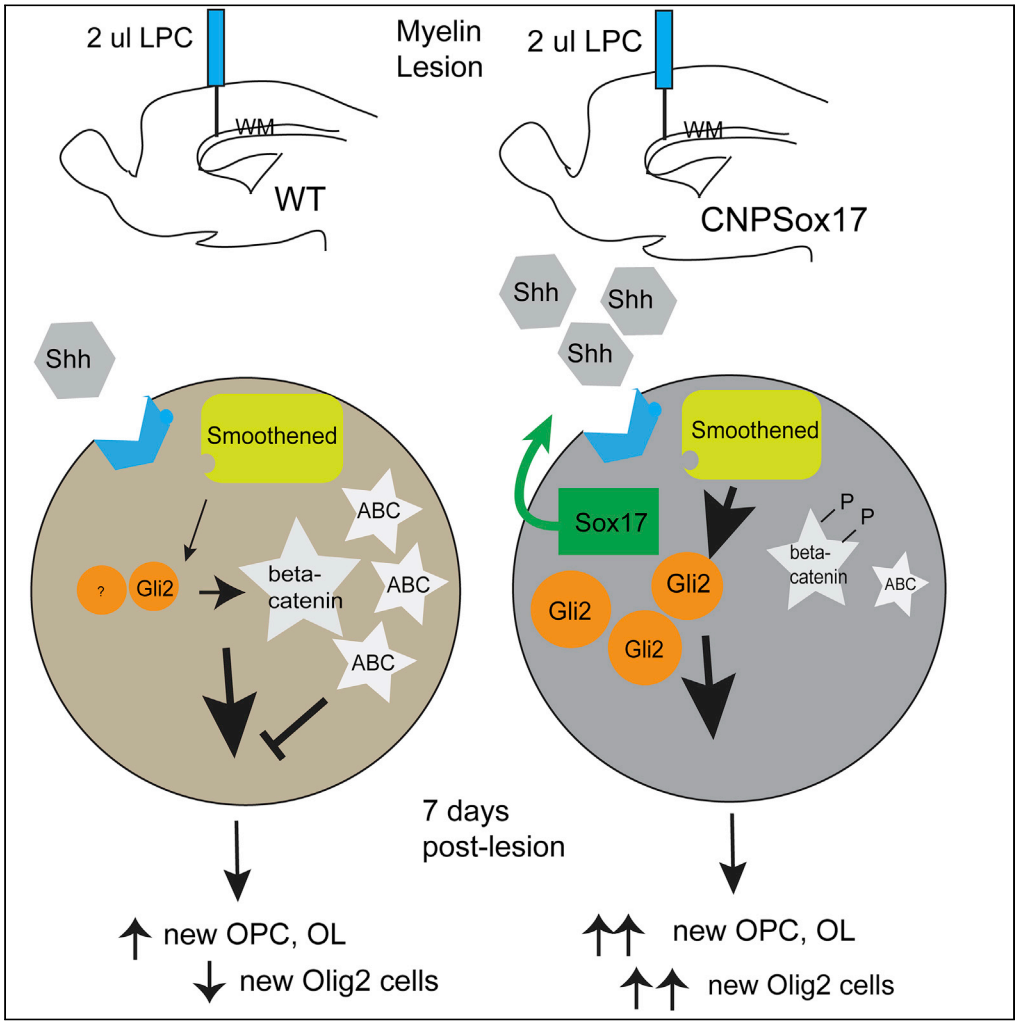


Xiaotian Ming, Jeffrey L. Dupree, Vittorio Gallo, Li-Jin Chew

vgallo@childrensnational.org (V.G.)
li-jin_chew@brown.edu (L.-J.C.)

## HIGHLIGHTS

Sox17 suppresses demyelination-induced Wnt/beta-catenin increase

Sox17 enhances Hedgehog signaling in adult white matter lesions

Adult Hedgehog-Smoothened activity promotes oligodendrocyte maintenance

Oligodendrocyte regeneration by Smoothened activation is Sox17 dependent

Ming et al., iScience *23*, 101592
October 23, 2020 
https://doi.org/10.1016/j.isci.2020.101592

iScience

CellPress
OPEN ACCESS

Article

# Sox17 Promotes Oligodendrocyte Regeneration by Dual Modulation of Hedgehog and Wnt Signaling

Xiaotian Ming,[1] Jeffrey L. Dupree,[2,3] Vittorio Gallo,[1,5,*] and Li-Jin Chew[1,4,*]

## SUMMARY

**Signaling pathways that promote oligodendrocyte development improve oligodendrocyte regeneration and myelin recovery from demyelinating pathologies. Sox factors critically control myelin gene expression and oligodendroglial fate, but little is known about signaling events underlying Sox-mediated oligodendroglial regeneration. In this study of the SoxF member Sox17, we demonstrate that Sox17-induced oligodendrocyte regeneration in adult myelin lesions occurs by suppressing lesion-induced Wnt/beta-catenin signaling which is inhibitory to oligodendrocyte regeneration and by increasing Sonic Hedgehog/Smoothened/Gli2 activity. Hedgehog signaling through Smoothened critically supports adult oligodendroglial viability and is an upstream regulator of beta-catenin. Gli2 ablation in adult oligodendrocyte progenitor cells indicates that Gli2 regulates beta-catenin differentially in wild-type and Sox17-overexpressing white matter. Myelin lesions in Sox17-deficient mice show beta-catenin hyperactivation, regenerative failure, and loss of oligodendrogenesis, despite exogenous Hedgehog stimulation. These studies indicate the benefit of Sox17 signaling targets to enhance oligodendrocyte regeneration after demyelination injury by modulating both Hedgehog and Wnt/beta-catenin signaling.**

## INTRODUCTION

Oligodendrogenesis is critically regulated by multiple signaling pathways, including canonical Wnt, Sonic hedgehog (Shh), Notch, and bone and morphogenetic proteins (BMP) (Fancy et al., 2014; Nicolay et al., 2007; Rowitch et al., 1999). The function of signaling mechanisms is well studied in oligodendrocyte (OL) development (Langseth et al., 2010; Merchan et al., 2007; Nery et al., 2001). However, signal regulation in the adult brain white matter (WM) is not fully understood (Guo et al., 2015; Samanta et al., 2015; Sanchez and Armstrong, 2018). Demyelinating pathologies are characterized by the failure of de novo OL generation by oligodendrocyte progenitor cells (OPCs) and reduced OL survival (Yeung et al., 2019). WM tissue damage induces spontaneous repair that is mediated by re-stimulation of morphogenic pathways such as Shh (Ferent et al., 2013), but aberrant signaling, such as Wnt, severely limits effective repair (Fancy et al., 2009), leading to exacerbation of disease. It is not known whether cross talk between Shh and Wnt operates in intact adult WM and during remyelination; understanding factors that control these interactions may aid strategies for repair. We hypothesize that the SRY-box containing (Sox) factor Sox17 promotes the integration of Shh-Wnt regenerative signaling pathways to facilitate OL production in WM lesions.

Sox transcription factors are evolutionarily conserved master regulators of development and organogenesis, with established effects on stem and progenitor cell generation and fate determination. Sox D (Potzner et al., 2007) and E (Stolt et al., 2002, 2003) members are among the best characterized ones for their involvement in oligodendroglial development. Sox F (7, 17, and 18), however, are predominantly endoderm and vascular determinants; only Sox17 is developmentally regulated in the oligodendroglial lineage, coincident with the onset of myelin gene expression and consistent with a role in cell differentiation (Sohn et al., 2006). Sox17 promotes OPC maturation to OLs in culture (Chew et al., 2011; Sohn et al., 2006), and, consistent with other Sox factors (Fan et al., 2018; Fu et al., 2010; Jia et al., 2010; Topol et al., 2009; Zorn et al., 1999), Sox17 serves as a Wnt signaling regulator in OPCs (Chew et al., 2011). WM lesions in multiple sclerosis and in rodent cuprizone demyelination models have shown that, despite its lack of expression in

[1]Center for Neuroscience Research, Children's National Research Institute, Children's National Hospital, Washington DC 20010, USA

[2]Department Anatomy and Neurobiol, Virginia Commonwealth Univ, Richmond, VA, USA

[3]Research Service, Hunter Holmes McGuire VA Medical Center, Richmond, VA 23249, USA

[4]Present address: Department of Molecular Biology, Cell Biology and Biochemistry, Brown University, Providence, RI 02903, USA

[5]Lead Contact

*Correspondence: vgallo@childrensnational.org (V.G.), li-jin_chew@brown.edu (L.-J.C.)

https://doi.org/10.1016/j.isci.2020.101592

intact adult WM, Sox17 protein is significantly upregulated in regenerating oligodendroglia (Moll et al., 2013). This strongly suggests Sox17 involvement in OL regeneration, an interpretation subsequently supported by studies of Sox17 ablation that abolished OL regeneration (Chew et al., 2019). These observations raise the possibility that increasing Sox17 levels *in vivo* may benefit WM repair by endogenous OPCs through mechanisms that regulate canonical Wnt signaling.

In our CNPSox17 transgenic mouse strain, where the mouse Sox17 cDNA fragment is expressed under the control of the *CNP* gene promoter (Ming et al., 2013; Yuan et al., 2002), we observe increased numbers of oligodendroglia in adult WM, as well as reduced vulnerability to demyelination damage (Ming et al., 2013). The adult WM of the CNPSox17 transgenic mouse contains increased numbers of NG2 OPCs along with CC1 OLs (Ming et al., 2013). Although increased Gli2 expression throughout the CNPSox17 oligodendroglial lineage was associated with increased survival of oligodendroglial cells, the mechanism by which Sox17 enhances oligodendrogenesis via hedgehog signaling and/or Wnt control is not defined (Ming et al., 2013). Our present analysis reveals the importance of adult hedgehog signaling in OL maintenance and implicates Sox17 as a dual regulator of Shh and Wnt signaling *in vivo*. In understanding Sox17 signaling, we find that potentiating hedgehog signaling facilitates lineage progression from the progenitor state during adult oligodendrogenesis and can overcome aberrant induction of canonical Wnt in WM pathology.

## RESULTS

### Sox17 Promotes OPC Differentiation at the NG2-O4 Transition

Our previous report showed that Sox17 overexpression in CNPSox17 mice sequentially promoted postnatal OL expansion (Ming et al., 2013). To elucidate the mechanism of Sox17 action in OL regeneration, we analyzed WM lesions generated in two lines of Sox17 mutants—Sox17-overexpressing (CNPSox17), and Sox17-deficient, CNPCre; Sox17f/f (Sox17CKO) mice.

In adult WM, analysis at 7 days post-lesion (DPL) (Figure 1A) shows that CNPCre-targeted Sox17 ablation (Sox17CKO) reduced the percentage of NG2+O4+/O4+ oligodendroglial cells (Figures 1A and 1B). Conversely, an increase in the percentage of doubly labeled NG2+/O4+ cells was found when Sox17 is overexpressed (CNPSox17, Figures 1C, 1D, and S1A). These observations suggest that Sox17 serves as a positive regulator across the NG2-O4 stage transition, suggesting that Sox17 promoted adult OPC differentiation and oligodendrogenesis, separately from its effect on OPC expansion per se (Chew et al., 2019). Sox17 deficiency also exaggerated the loss of CC1+ OLs in lesioned WM (Figure S1B), supporting the view that reduced formation of pre-myelinating O4 cells from NG2 OPCs would impair the regeneration of CC1 cells.

To determine whether Sox17-mediated oligodendrogenesis impacted myelin structure, electron microscopy confirmed that Sox17 overexpression in CNPSox17 prevented a significant reduction in myelinated axons at 7 DPL (Figures 1E and 1F). In contrast to Saline controls (Figures 1G and S1C WT-Sal vs CNPSox17-Sal), Lyso lesions produced greater changes in G-ratio parameters in WT than in CNPSox17 (Figures 1H and S1C WT-Lys vs CNPSox17-Lys). As myelin wraps were observed to separate from the axon after demyelination, an additional measurement of myelin thickness was made within myelinated axons. These measurements show significant overlap between mouse strains after Saline injection (Figure S1D), whereas myelin is significantly thicker in the CNPSox17-Lys relative to WT-Lys (Figure S1E), indicating the substantial effect of Sox17 overexpression in preserving myelin ultrastructure when challenged with myelin damage. We had previously found increased cell survival in lesions generated in CNPSox17 mice (Ming et al., 2013), suggesting a protective property of Sox17 overexpression. Based on these findings, we hypothesize that increased de novo oligodendrogenesis, aided by cell and myelin protection, contributes to attenuated myelin damage.

### Sox17 Overexpression Enhances De Novo Regeneration of Oligodendroglia

In order to determine whether Sox17-mediated changes in adult oligodendroglial regeneration are the result of increased OPC differentiation, we ablated Sox17 in PDGFR-expressing OPCs in P60 PDGFRcre; Sox17f/f (Sox17PCKO) mouse mutants and analyzed WM lesions at 7 DPL. This showed that CC1 OL cells were decreased after Sox17 ablation in Sox17PCKO WM lesions (Figures 2A and 2B). To determine whether newly formed OLs were increased in adult CNPSox17 WM, we performed Bromodeoxyuridine (BrdU) pulse labeling in intact and lesioned WM according to the paradigm illustrated in Figure 2C. The numbers of BrdU-labeled cells (Figure S1F) and BrdU-labeled Olig2+ cells (Figures 2D and 2E) were significantly

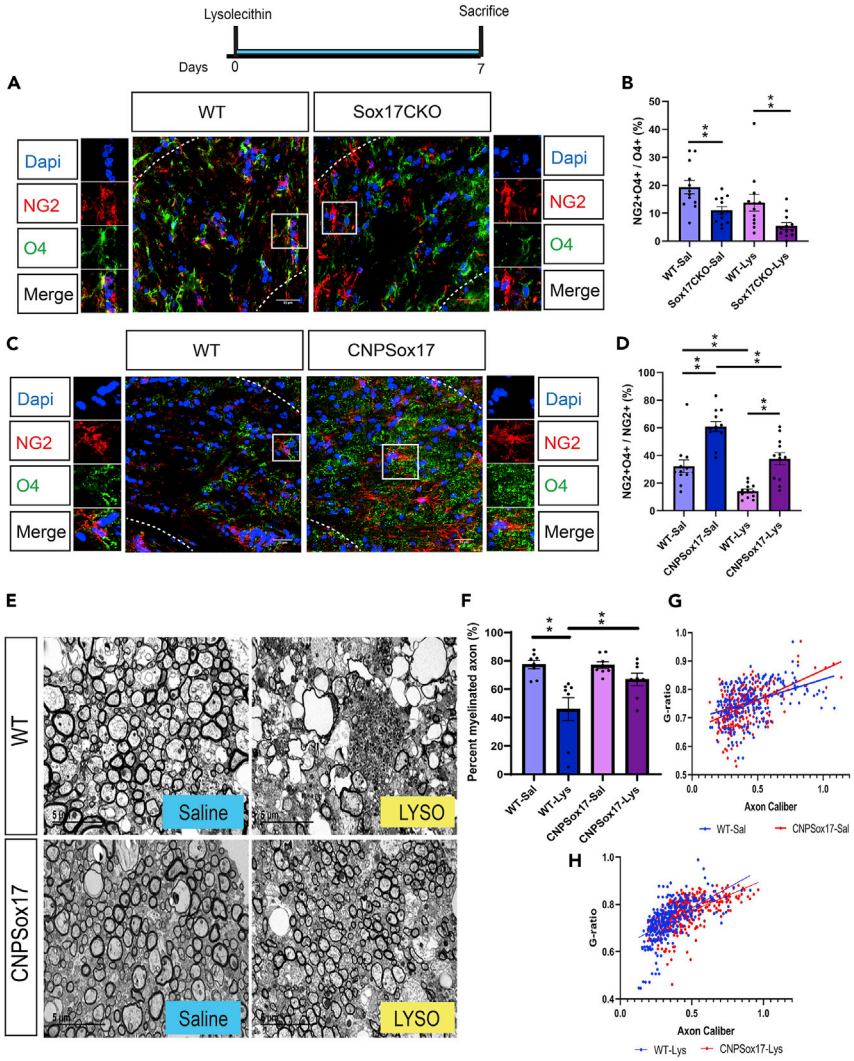


**Figure 1. Sox17 Regulates Adult Oligodendrogenesis and Attenuates Lesion-Induced Changes in Myelin Ultrastructure**

(A) Confocal images showing NG2(red) and O4(green) dual-labeled cells in P60 Sox17CKO WM lesions at 7 days post-lesion (7DPL). Scale bar = 25 um.

(B) Quantitative analysis of cells in Sox17CKO at the NG2+O4+ transition at 7 DPL, expressed as a percentage of total O4+ cells. Values are mean + SEM. **p < 0.01; two-way ANOVA analysis.

(C) Confocal images showing NG2 (red) and O4 (green) dual-labeled cells in P60 CNPSox17 WM lesions at 7DPL. Scale bar = 25 um.

(D) Quantitative analysis of cells in CNPSox17 at the NG2-O4 transition at 7 DPL, expressed as a percentage of total NG2 cells. Values are mean ± SEM. **p < 0.01; two-way ANOVA analysis.

(E) Electron microscopy images showing Sox17 overexpression (CNPSox17) dramatically reduces lysolecithin (LYSO)-induced changes in myelination at 7 DPL. Scale bar = 5 um.

(F) The percent of myelinated axons (%) in intact (Sal) or lesioned (Lys) WM of WT and CNPSox17. *p < 0.05, **p < 0.01; two-way ANOVA analysis.

(G) Regression analysis of G-ratio plot against axon caliber of intact (Sal) WT and CNPSox17 callosal WM, showing extensive overlap.

(H) Regression analysis of G-ratio plot against axon caliber of lesioned (Lys) WT and CNPSox17 WM, showing separation of G-ratio values. N = 4. *p < 0.05, **p < 0.01; two-way ANOVA analysis. Dashed lines delineate the confines of the WM area outside the edge of the injection site.

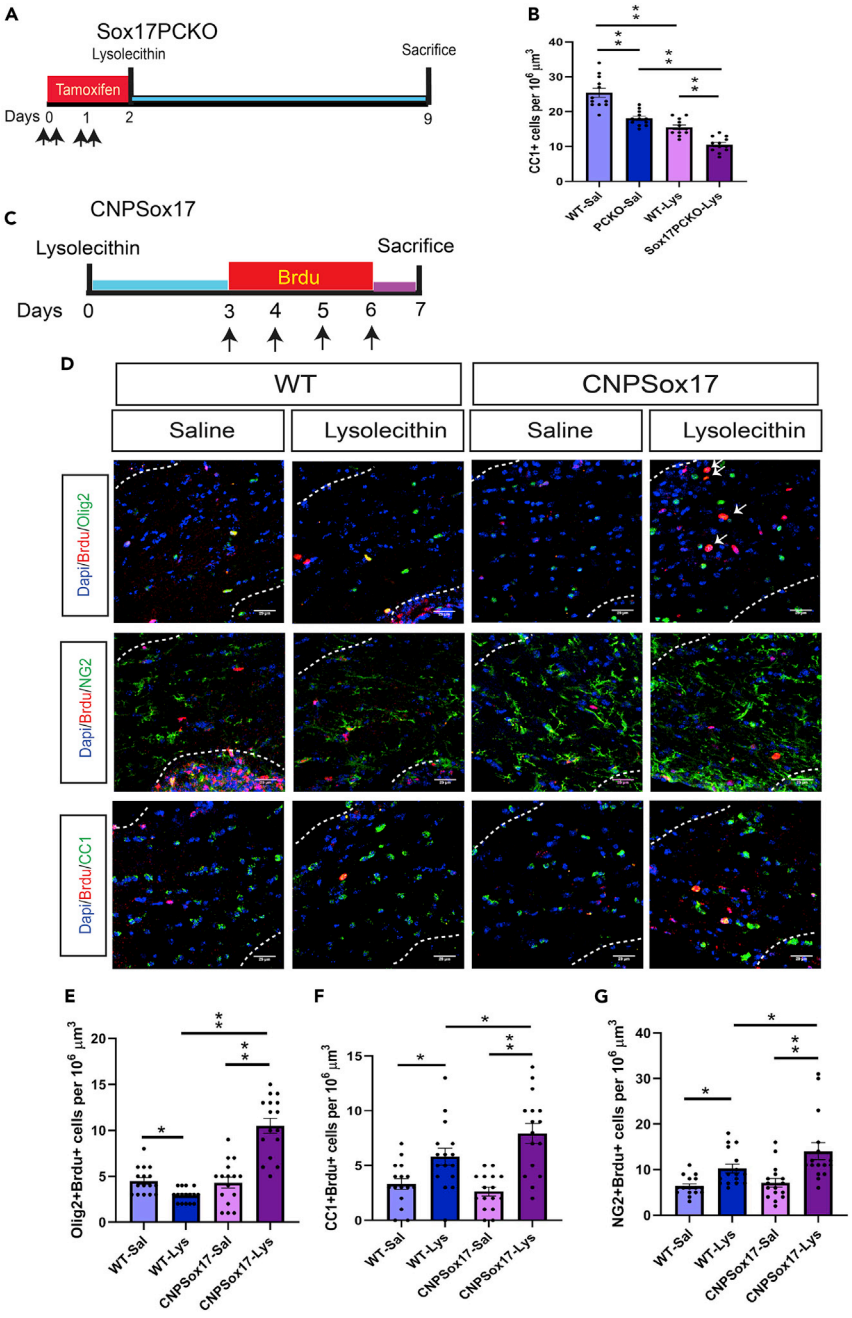


**Figure 2. Sox17 Promotes Production of New Oligodendrocyte Cells at 7 DPL**

(A) Schematic diagram illustrating the tamoxifen and lysolecithin injection paradigm to genetically ablate Sox17 in Sox17PCKO. Arrowheads indicate each tamoxifen injection.

(B) Quantitative analysis showing reduced CC1 oligodendrocyte production in adult Sox17PCKO at 7DPL. Values are mean + SEM. **p < 0.01; two-way ANOVA analysis.

(C) Schematic diagram illustrating stereotaxic lysolecithin injection and daily i.p. 50mg/kg Brdu pulse chase (arrowheads) between days 3-6 before sacrifice at 7DPL.

(D) Confocal microscope images of Brdu+(red) labeling of Olig2+(green), NG2+(green), and CC1+(green) cells in intact (saline) or lesioned (Lysolecithin) WM of WT and CNPSox17 subcortical WM. Scale bars = 29 um.

(E) Newly formed Olig2 cells (Olig2+Brdu+) decrease in WT lesions, but increase in CNPSox17 lesions. Values are mean + SEM. *p < 0.05, **p < 0.01; two-way ANOVA analysis.

(F) WM damage stimulates more newly formed CC1+ oligodendrocytes in CNPSox17 lesions. Values are mean + SEM. *p < 0.05, **p < 0.01; two-way ANOVA analysis.

**Figure 2. *Continued***
(G) WM damage stimulates more newly generated NG2+ progenitor cells (NG2+Brdu+) in CNPSox17 lesions. Cell density values are mean ± SEM obtained from 4 independent litters. *p < 0.05, **p < 0.01; two-way ANOVA analysis. Dashed lines delineate the confines of the WM area outside the edge of the injection site.

increased, indicating enhanced de novo generation of oligodendroglia. The numbers of newly formed CC1+ OLs (Figure 2F) and nascent NG2+ OPCs (Figure 2G) were also increased in CNPSox17 lesions. Interestingly, we observed a decline in the total number of Ki67 + cells in CNPSox17 (Figure S1G), suggesting that Sox17 promoted cell cycle exit and terminal OPC differentiation. This is supported by increased Ki67 + cells in both strains of intact Sox17-deficient mutants (Figures S1H and S1I, Sal). In the CNPSox17 transgenic mouse, the continuous generation and differentiation of OPCs is consistent with our observation of increased NG2 OPCs in the CNPSox17 mouse even at P120 (Figure S1J–S1K).

## Sox17 Attenuates Beta-Catenin Activation in Lysolecithin Lesions

Since canonical Wnt inhibition was previously shown to benefit OPC differentiation and remyelination (Fancy et al., 2009) and Sox17 regulates Wnt/beta-catenin signaling in developing OPCs (Chew et al., 2011), we sought to understand Sox17-mediated changes in the canonical Wnt effector, beta-catenin (Figure S2A) in the context of WM lesions. As previously reported (Fancy et al., 2009), the numbers of cells expressing beta-catenin increase dramatically in WT controls after lysolecithin lesion. This increase in beta-catenin-expressing cells was attenuated in CNPSox17 at 3 DPL and abolished by 7 DPL (Figures 3A and 3B). As beta-catenin accumulation results from downregulation of its phosphorylation (Figure S2A), we analyzed its phosphorylation status. The effect of Sox17 on active or unphosphorylated beta-catenin (ABC) was more striking (Figures 3A and 3C), showing no significant increase at both time points. The change of ABC within Olig2+ cells also reflects suppression of lesion-induced beta-catenin activation by Sox17 (Figure 3D). While the proportion of ABC + cells that were Olig2+ oligodendroglia was lower with Sox17, the fraction of total oligodendroglial ABC + cells responding to demyelination was not affected by Sox17 (Figure S2B). These observations indicate that Sox17 serves to prevent beta-catenin activation in oligodendroglia after demyelination injury.

We observed in P30 tissue lysates that while the levels of total b-catenin in CNPSox17 WM was higher than WT, ABC was not correspondingly increased (Figures 3E and 3F), leading to decreased ABC/beta-catenin ratios (WT 5.734 ± 0.062 vs CNPSox17 1.157 ± 0.059). The increase in Axin2 (Figures 3E and 3F) suggests turnover, so we determined differences in beta-catenin phosphorylation state in WM lesions. We observed lower levels of P-beta-catenin S33/S37/T41 in P60 lysolecithin lesions of Sox17CKO (Figures 3G and 3H). Consistent with this, lysolecithin demyelination in CNPSox17 WM induced a quantitatively larger increase in cells positive for P-beta-catenin S33/S37/T41 (Figures 3I and 3J). Sox17 ablation in Sox17CKO and Sox17PCKO inherently raised the numbers of beta-catenin-expressing cells (Figures S2C and S2D, WT-Sal vs Sox17CKO-Sal or Sox17PCKO-Sal) and upregulated ABC (Figures 3K and 3L). The pattern of beta-catenin changes in Sox17CKO and Sox17PCKO (Figures S2C and S2D) reflects that of ABC (Figures 3K and 3L), suggesting that the levels of beta-catenin may be low in the absence of Sox17. This indicates that Sox17 represses ABC + cells *in vivo*. These support the notion that Sox17 prevents beta-catenin activation by increasing its phosphorylation, particularly in WM lesions.

## Sox17 Increases Cellular Sonic Hedgehog Localization and Activity

Although we had previously found that Sox17 protein formed a complex with beta-catenin in developing OPCs (Chew et al., 2011), the effect of Sox17 on beta-catenin destabilization in regenerating oligodendroglia *in vivo* is likely to be indirect. Based on our finding of Wnt antagonist Secreted Frizzled-Related Protein (SFRP), a hedgehog target (Katoh and Katoh, 2006) among regulated genes of Sox17 (Chew et al., 2011), and an increased number of Gli2-expressing cells in CNPSox17 WM, we considered the possibility of Shh involvement (Figure S2E) in Sox17-induced oligodendrogenesis. Immunoprecipitation assays failed to detect complex formation between Sox17 and beta-catenin in adult WM (Figure S2F). Instead, Sox17 was found in WM complexes containing Oct4 (Figure S2F). Interestingly, Gli2 is found in Oct4 complexes (Figure S2F). The lack of interaction between Sox17 and beta-catenin was confirmed by immunoprecipitation with beta-catenin antibodies (Figure S2G). The presence of Oct4 in Olig2-expressing cells of adult WM suggests an OL progenitor state that is enhanced in adult CNPSox17 WM (Figure S2H), which may encourage molecular interactions between Oct4 and Sox17.

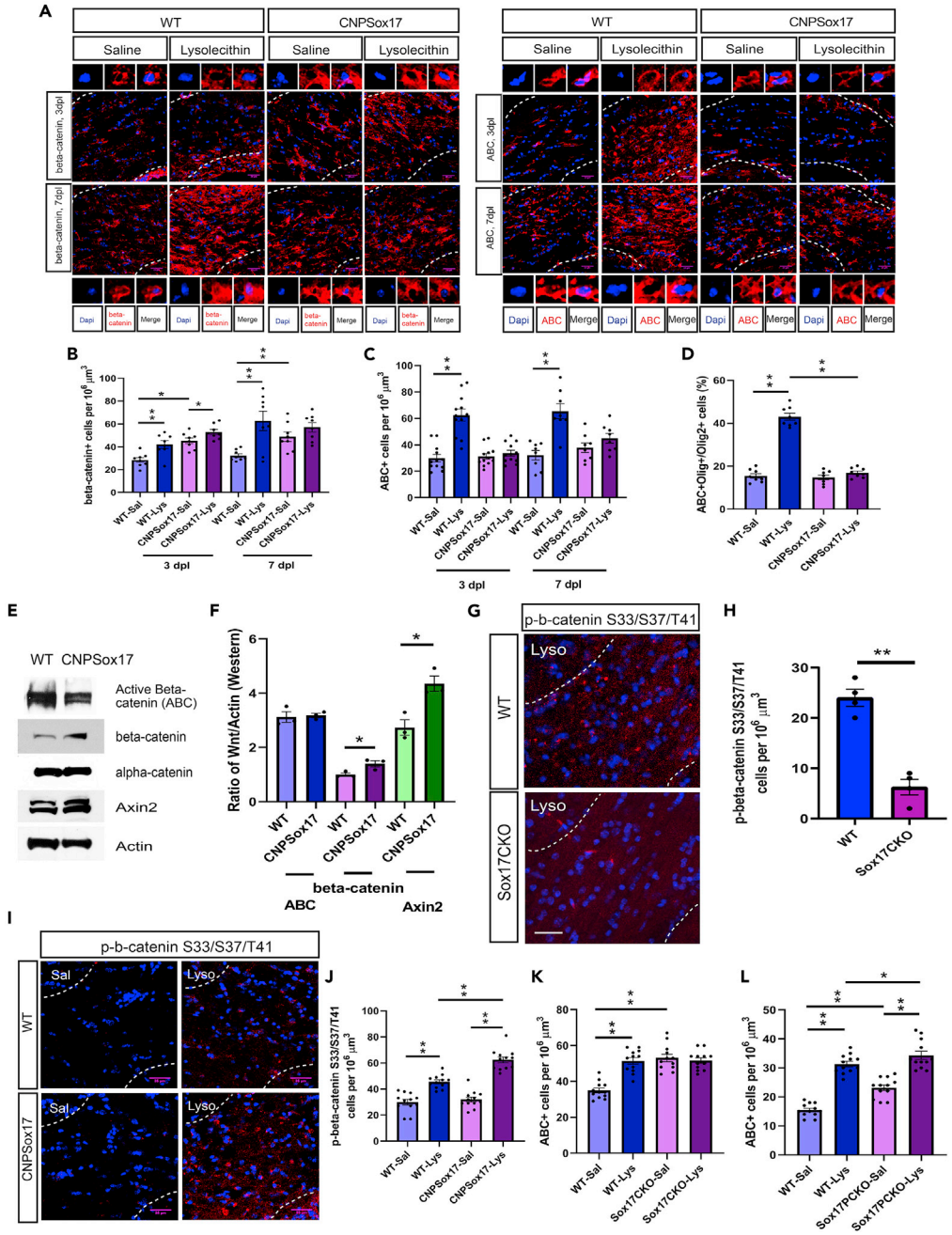


**Figure 3. Sox17 Regulates Beta-Catenin Accumulation and Activation**

(A) Confocal images showing beta-catenin (red) or ABC+ (red) in WM lesions of WT or CNPSox17. Scale bar = 29 um.

(B and C) (B) Quantitative analysis of beta-catenin+ (B) or ABC+ (C) cells in WT or CNPSox17 WM at 3 or 7 DPL. Values are mean + SEM. *p < 0.05, **p < 0.01; two-way ANOVA analysis.

(D) Sox17 overexpression prevents lesion-induced change in the percentage of Olig2+ cells expressing ABC. Values are mean + SEM. **p < 0.01; two-way ANOVA analysis.

(E) Western blot analysis of ABC, beta-catenin, alpha-beta-catenin, and Axin2 in intact WM of WT and CNPSox17 WM (P30).

(F) Relative abundance of ABC, beta-catenin, and Axin2 levels from Western blots expressed as ratio over Actin. Values are mean + SEM; Student's T-test.

(G) Confocal microscope images of p-beta-catenin S33/S37/T41-expressing cells in WT and Sox17CKO Lyso lesions at 7 DPL. Scale bar = 20 um.

**Figure 3. *Continued***

(H) Quantitative analysis of p-beta-catenin S33/S37/T41-expressing cells at 7 DPL. Values are mean + SEM. **p < 0.01; Student's T-test.

(I) Confocal microscope images of p-beta-catenin S33/S37/T41 at 3 DPL. Scale bar = 35 um.

(J) Quantitative analysis of p-beta-catenin S33/S37/T41-expressing cells at 3 DPL. Values are mean + SEM. **p < 0.01; two-way ANOVA analysis.

(K) Sox17 ablation increases ABC + cells in Sox17CKO. Values are mean + SEM. **p < 0.01; two-way ANOVA analysis.

(L) ABC + cells are increased in intact and lesioned Sox17PCKO WM. Values are mean and SEM obtained from 3 independent litters. *p < 0.05, **p < 0.01; two-way ANOVA analysis. Dashed line(s) delineate the WM area outside the edge of the injection site.

Our previous report described increased Gli2 throughout postnatal WM development in CNPSox17 and which, unlike in WT lesions, did not decrease with demyelination in CNPSox17 (Ming et al., 2013). This indicates that intrinsically elevated Gli2 signaling arising from Hedgehog may be involved in beta-catenin control. We therefore investigated the role of Hedgehog signaling stimulated by Sox17. Histological analysis showed Shh immunoreactivity was increased in lesions of WT (Figures 4A and 4B). However, in CNPSox17, where basal levels were already elevated, no further increase is observed in lesions (Figures 4A and 4B). This is similar to the reported pattern of Gli2 expression in CNPSox17 (Ming et al., 2013). The density of cells doubly labeled with Shh and Olig2 cells increased in both WT and CNPSox17 lesions (Figure S3A); however, the percentage of Olig2 cells associated with Shh was clearly increased in CNPSox17 over WT (Figure 4C). The induction of Shh + cells which are oligodendroglia in response to demyelination was decreased in CNPSox17, likely from reduced damage (Figure S3B). This suggests that Sox17 overexpression supported increased Shh co-localization in the oligodendroglial lineage, which could enhance regenerative signaling.

## Hedgehog Regulates Beta-Catenin and Not Vice Versa

To understand the relationship between innate Shh and Wnt/beta-catenin activation, we used stereotaxic injections of the Smoothened antagonist, cyclopamine or Wnt antagonist, CCT036477 (CCT) into adult WM to determine the response of pathway mediators. Injection of CCT did not alter Gli2-expressing cells in WM of both WT and CNPSox17 strains in 1 or 3 day post-injection (dpi) (Figure S3C). CCT decreased beta-catenin-, ABC-, and BATGAL LacZ-expressing cells (Figures S3D–S3F) without altering Shh-expressing cells (Figure S3G), indicating that either the pathways did not interact or Shh/Gli2 may instead act upstream of beta-catenin. Indeed, stereotaxic injection of 5 um of the Smoothened antagonist cyclopamine downregulated the number of cells expressing Gli2 (Figure 4D), beta-catenin, and active-beta-catenin (ABC) at 1 dpi (Figures 4E and 4F), indicating positive regulation of canonical Wnt by Hedgehog. Subsequent increases in both beta-catenin and ABC-expressing cells (Figures 4E and 4F) at 3 dpi suggest a regenerative response to possible cell loss. Stereotaxic injection of cyclopamine in BATGAL and CNPSox17; BATGAL hybrids reduced LacZ cells in adult WM, indicating that Hedgehog/Smoothened activity supported beta-catenin signaling (Figure 4G). In view of observed cell maintenance effects of Smoothened, it is likely that cyclopamine also regulated cell survival (see Figure 6). Like CCT, this dose of cyclopamine did not affect Shh levels in the WM (Figure S3H).

## Sox17 Modulates Beta-Catenin Response to Changes in Gli2

Since canonical Wnt/b-catenin is regulated in cells of the oligodendroglial lineage and Gli2 was previously found to be elevated in CNPSox17 (Ming et al., 2013), we hypothesized that changes in Gli2 could modulate beta-catenin in adult WM cells. We first investigated whether changes in endogenous Sox17 regulated Gli2 and found that Sox17 ablation lowered endogenous Gli2 and Olig2+ cells (Figures S4A and S4B). To understand the role of Hedgehog/Gli2 in adult WM, we performed targeted Gli2 ablation in adult OPCs using PDGFRaCre-ERT2 in WT and CNPSox17 WM (Figure 5A). Gli2+ cells were significantly reduced in both intact and lesioned WM of WT and CNPSox17 at 3 dpl (Figures S4C and S4D, Gli2f/f). In WM lesions (Lys), Gli2 ablation led to a decline in Olig2+ cells in both WT and CNPSox17 (Figures 5B and 5C), indicating a requirement for Gli2 in the production or maintenance of the oligodendroglial lineage in repair. It is noteworthy that Gli2 ablation in CNPSox17 lesions decreases Olig2+ cells to WT levels, as it indicates that Gli2 mediates CNPSox17-induced oligodendrogenesis. The changes in CC1 OLs in lesions suggest differential roles for Gli2, i.e., in CNPSox17 lesions, and Gli2 supports OL production (Figures 5D and 5E), while the increased CC1 cells in WT lesions suggest inhibitory role for Gli2 in OPC differentiation. As beta-catenin and ABC levels fall in the absence of Gli2 in WT lesions (Figures 5F and 5G), the observations are consistent with the notion that Hedgehog-Gli2 signaling in WT preferentially supports positive regulation of beta-catenin in less mature stages of the OL lineage. We find that, in WT lesions, NG2+ (Figures S4E and S4F) and

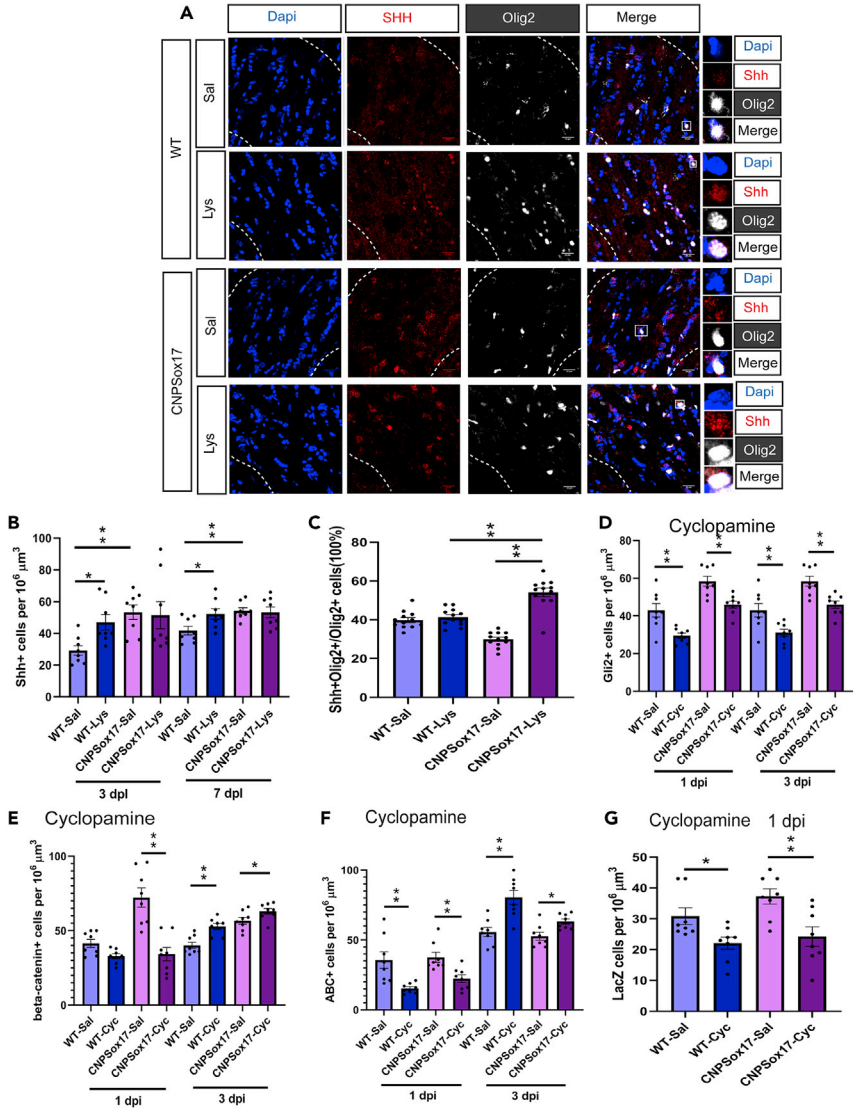


**Figure 4. Sox17 Regulates Shh Levels and Activity in Adult WM**

(A) Confocal microscope images of Shh+(red) and Olig2+(white) cells in P60 WT and CNPSox17 WM at 3 DPL. Scale bar = 20 um.

(B and C) (B) Quantitative analysis of total Shh + cells at 3 or 7 DPL (C) Percentage of total Olig2+ cells associated with Shh is selectively increased in CNPSox17 lesions (Lys) at 3 DPL. Values are mean + SEM. *p < 0.05, **p < 0.01; two-way ANOVA.

(D) Quantitative analysis of Gli2+ cells in WT and CNPSox17 WM at 1 or 3 dpi after stereotaxic injection with 2 ul of 5 uM cyclopamine (Cyc) into subcortical WM, showing effective Gli2+ cell decrease. Values are mean + SEM. **p < 0.01; two-way ANOVA.

(E) Quantitative analysis of beta-catenin+ cells in WM of WT and CNPSox17 strains at 1 or 3 dpi after stereotaxic administration of 2 ul of 5 uM cyclopamine. Values are mean + SEM. *p < 0.05, **p < 0.01; two-way ANOVA.

(F) Quantitative analysis of ABC + cells in WM of WT and CNPSox17 strains at 1 or 3 dpi after stereotaxic administration of 2 ul of 5 uM cyclopamine. Values are mean + SEM. *p < 0.05, **p < 0.01; two-way ANOVA.

(G) Quantitative analysis of LacZ + cells in intact WM of Bat-Gal and CNPSox17; Bat-Gal strain at 1 day post-injection (dpi) with 5 uM cyclopamine. Values are mean ± SEM. N = 3 independent litters. *p < 0.05, **p < 0.01; two-way ANOVA analysis. Dashed line(s) delineate the WM area outside the edge of the injection site.

O4+ (Figures S4E and S4G) cells decline with Gli2 ablation, but not CC1 (Figure 5E). In contrast, in CNPSox17 lesions, a role for Gli2 in promoting OPC differentiation is observed (Figure 5E CC1, Lys, Figures S4E–S4G).

In the intact WT WM (Sal), Figures 5F and 5G reveal a positive role for Gli2 in beta-catenin accumulation and activation (ABC), while in CNPSox17, Gli2 no longer served as an activator of beta-catenin and ABC. In intact

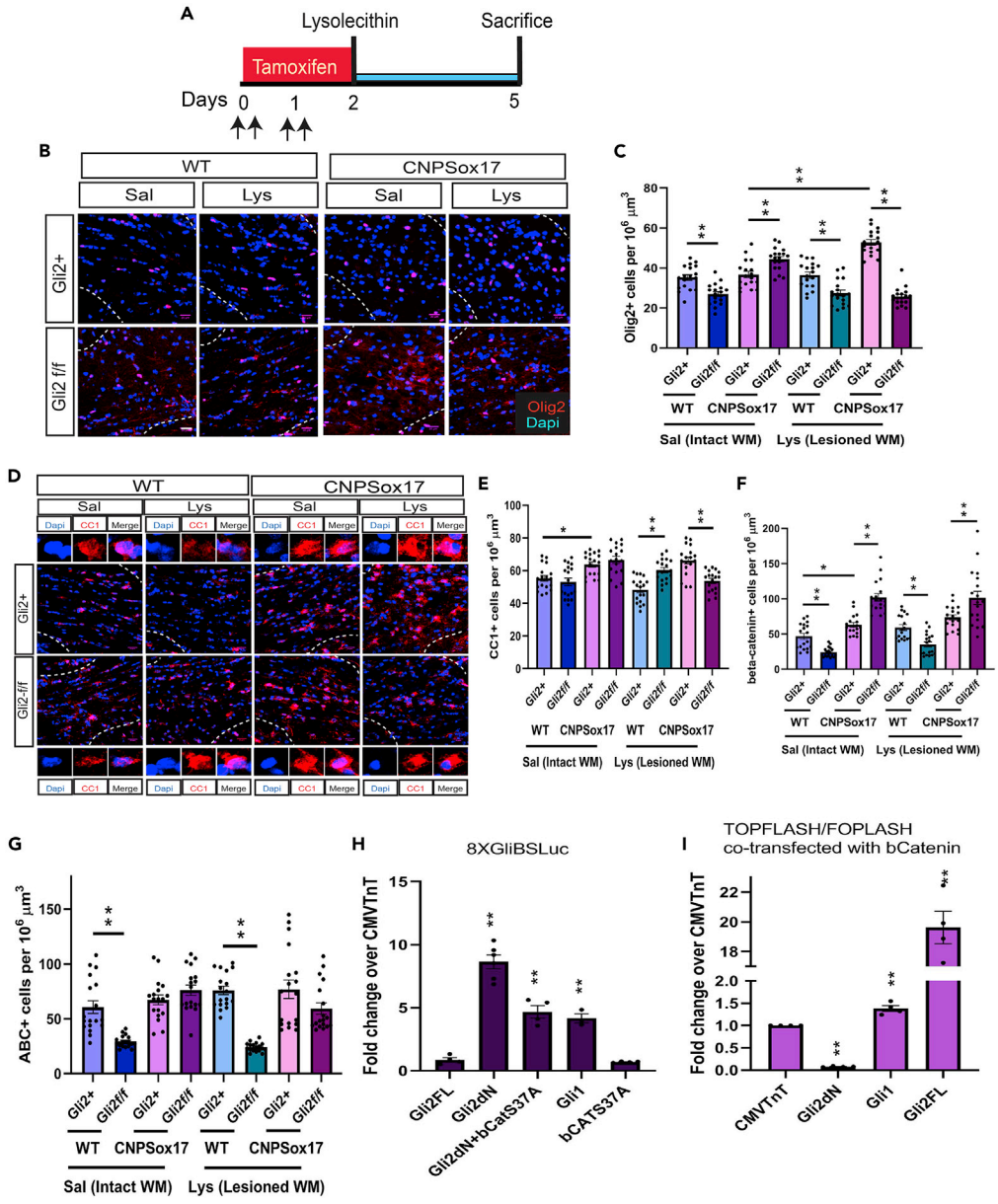


**Figure 5. Sox17 Alters Gli2-Mediated Regulation of Beta-Catenin**

(A) Illustration of tamoxifen induction paradigm to generate targeted Gli2 ablation in adult PDGFRaCre-ERT2; Gli2f/f or PDGFRaCre-ERT2; Gli2f/f; CNPSox17 (CNPSox17; Gli2f/f) OPCs within Lyso lesions. Analysis was performed at 3 DPL.

(B) Confocal images of Olig2 cells (red) following Gli2 ablation (Gli2f/f). Scale bar = 20 um.

(C) Quantitative analysis of cells expressing Olig2 following Gli2 ablation. Values are mean + SEM. *p < 0.05, **p < 0.01; two-way ANOVA analysis.

(D) Confocal images of CC1 cells (red) following Gli2 ablation. Scale bar = 20 um.

(E) Quantitative analysis of CC1 cells following Gli2 ablation. Values are mean + SEM. *p < 0.05, **p < 0.01; two-way ANOVA analysis.

(F) Quantitative analysis of immunohistochemical changes in beta-catenin-expressing cells in intact (Sal) and lesioned (Lys) WM following genetic Gli2 ablation (Gli2f/f) in PDGFRaCre; Gli2ff (WT) or PDGFRaCre; Gli2ff; CNPSox17 (CNPSox17) mice. Gli2+ are Gli2-expressing controls. Values are mean + SEM. *p < 0.05, **p < 0.01; two-way ANOVA analysis.

(G) Quantitative analysis of cells expressing ABC following Gli2 ablation. Values are mean + SEM; two-way ANOVA, *p < 0.05, **p < 0.01.

(H) *In vitro* luciferase reporter assays in HEK293 cells to determine transcriptional activity of GLI2FL (full length) and Gli2dN (N-terminus deleted) expression vectors at a Gli-responsive element (8XGliBSLuc). Active-beta-catenin

**Figure 5. *Continued***

(bCatS37A) does not stimulate GliBS reporter activity. Values are fold change in luciferase activity relative to Controls consisting of 8XGliBSLuc co-transfected with CMVTnT vector. Values are mean ± SEM, N = 3 experiments. Only GLI2FL and bCATS37A are not significantly different from each other. One-way ANOVA, Holm-Sidak post-hoc test. **$p < 0.01$.

(I) Luciferase reporter assays in a human oligodendroglioma cell line reveal differential regulation by GLI2FL (full length) and Gli2dN (N-terminus deleted) expression vectors at a TCF/beta-catenin-responsive element (TOPFLASH). TOPFLASH or FOPFLASH plasmids were transfected with beta-catenin and co-transfected with CMVTnT vector or GLI plasmids. Relative activity is expressed as fold change of TOPFLASH/FOPFLASH ratios over TOPFLASH/FOPFLASH ratio for CMVTnT + beta-catenin. Values are mean ± SEM. N = 4 experiments. Gli2dN, Gli1 and Gli2FL were significantly different from CMVTnT. One-way ANOVA, Holm-Sidak post-hoc test. **$p < 0.01$. Dashed line(s) delineate the WM area outside the edge of the injection site.

tissue, Gli2 ablation in CNPSox17 did not decrease NG2+ OPCs and O4+ cells (Figures S4F and S4G), showing instead enhanced lineage progression by Gli2 (Figures S4F and S4G). Taken together, our observations support the interpretation that high levels of Sox17 uncouple Gli2 from its positive regulation of beta-catenin.

As we hypothesize that changes in Gli2 activation status may mediate these observations in WM, we explored the possibility that constitutively active Gli2 may impact beta-catenin/TCF transcriptional levels in reporter assays as an indirect readout of cross talk. We first compared the activities of recombinant Gli2 constructs using a Gli-responsive enhancer and confirmed a dramatic increase in transcriptional activity in the absence of its N-terminal repressor domain (Gli2dN) over its full-length protein (Gli2FL) (Figure 5H). We then analyzed the effect of recombinant, active Gli2 on beta-catenin/TCF-responsive enhancers using TOPFLASH/FOPFLASH reporters. Gli2dN and Gli2FL each alone does not stimulate TCF/beta-catenin-dependent basal TOPFLASH regulatory activity like beta-catenin (bCatenin) and constitutively active-beta-catenin (bCATS37A) (Figure S4H). However, when co-transfected with bCatenin in cultured human oligodendroglioma cells, where both Hedgehog and Wnt signaling are implicated (Takezaki et al., 2011), constitutively active Gli2dN selectively represses TOPFLASH/FOPFLASH promoter activity compared with Gli2FL (Figure 5I), indicating that active Gli2 was able to repress beta-catenin activity, while full-length Gli2 was ineffective in suppression. This suggests the possibility that changes in canonical Hedgehog activity bear the potential to modulate canonical Wnt output.

## Smoothened Is Required for Adult Oligodendroglial Lineage Maintenance and Sox17-Mediated Oligodendrogenesis

To determine whether the effects of Gli2 ablation could be in part mediated by changes in canonical Hedgehog signaling, we analyzed the cellular effect of Smoothened ablation in PDGFRa-expressing OPCs of the adult WM. Consistent with a role in oligodendroglial lineage cell generation and homeostasis, tamoxifen-induced SMO ablation via PDGFRaCre-ERT2 (Figures 6A, S5A, and S5B) results in decreased Gli2-expressing cells (Figures 6B and S5C). Interestingly, the function of Smoothened on beta-catenin and ABC does not distinguish CNPSox17 from WT. Figures 6C and 6D both show SMO as a positive regulator of beta-catenin and ABC, as SMO ablation decreases beta-catenin and ABC levels in PDGFRaCre-ERT2; Smof/f (WT; SMOf/f) and PDGFRaCre-ERT2; Smof/f; CNPSox17 (CNPSox17; SMOf/f). We considered the possibility that oligodendroglial abnormalities or pathology may explain these observations. Indeed, in the absence of SMO, Olig2+ (Figures 6E and S5D), O4+ and CC1 oligodendroglial cells were negatively impacted (Figures 6F–6H, S5E, and S5F). Acute cyclopamine administration led to decreased Olig2 immunoreactivity (Figure S5G), suggesting events preceding Olig2 cell loss. Furthermore, SMO ablation decreases nuclear distribution of Ki67 (Figure S5H). Interestingly, we observe an increase in total Ki67 + cells (Figure S5I) in these mutants, indicating that the majority of Ki67 + cells in Smo-deficient mice show abnormal, non-nuclear Ki67 intracellular distribution (Figure S5J). The response to OL cell loss in WM tissue includes the recruitment of NG2+ cells (Figure 6I) which display hypertrophy (not shown) and shortened processes (Figure S5K) similar to those reported after injury (Dimou and Gallo, 2015).

In support of a role for SMO in cell survival, we observed increased cleaved caspase-3-labeled cells by immunocytochemistry when SMO is ablated (Figure 6J). Adult CNPSox17 WM was previously found to exhibit enhanced resistance to lesion-induced cell death (Ming et al., 2013). SMO ablation abolished the protective effect of Sox17 overexpression in both intact and lesioned WM in CNPSox17 (Figure 6K). Furthermore, the inhibition of Smoothened activity with cyclopamine in lesions did not alter caspase-3 in WT lesions where it is inherently high, but cyclopamine significantly increased cleaved caspase-3 in lesions of the CNPSox17 (Figures 6L–6M). These

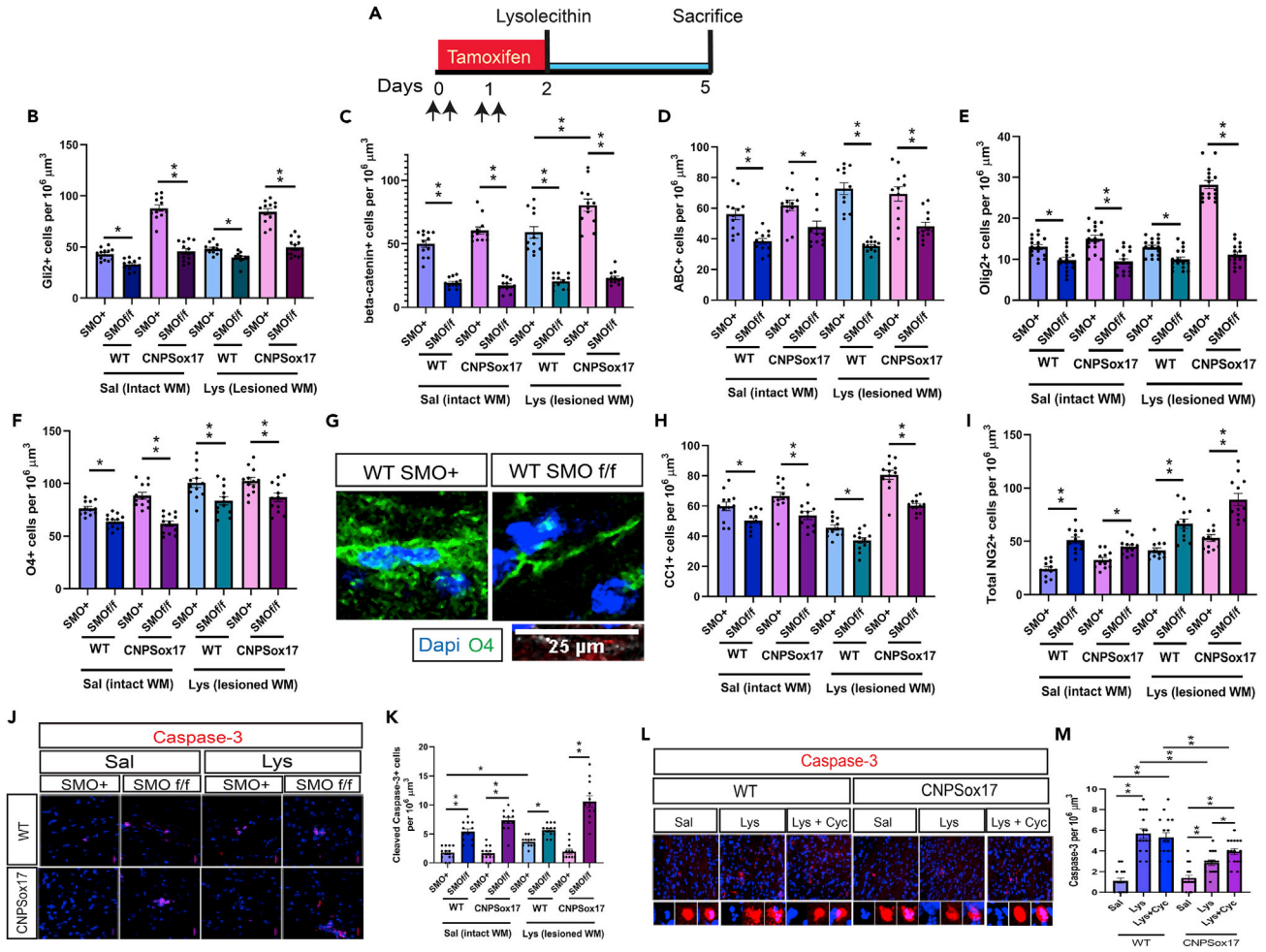


**Figure 6. Smoothened Is Required for Oligodendroglial and Beta-Catenin Maintenance**

(A) Illustration of tamoxifen induction paradigm to generate targeted Gli2 ablation in adult OPCs within Lyso lesions. Analysis was performed at 3 DPL.

(B) Quantitative analysis by showing immunocytochemical changes in Gli2-expressing cells in intact(Sal) and lesioned(Lys) WM following genetic SMO ablation (SMOf/f) in PDGFRaCre; SMOff (WT) or PDGFRaCre; SMOff; CNPSox17 (CNPSox17) mice at 3 DPL. SMO-expressing control groups are indicated by SMO+. Values are mean + SEM. *p < 0.05, **p < 0.01; two-way ANOVA analysis.

(C) Quantitative analysis of cells expressing beta-catenin following SMO ablation. Values are mean + SEM. *p < 0.05, **p < 0.01; two-way ANOVA analysis.

(D) Quantitative analysis of cells expressing ABC + cells following SMO ablation. Values are mean + SEM. *p < 0.05, **p < 0.01; two-way ANOVA analysis.

(E) Quantitative analysis of cells expressing Olig2+ cells following SMO ablation. Values are mean + SEM. *p < 0.05, **p < 0.01; two-way ANOVA analysis.

(F) Quantitative analysis of cells expressing O4+ cells following SMO ablation. Values are mean + SEM. *p < 0.05, **p < 0.01; two-way ANOVA analysis.

(G) Images showing loss of O4 immunoreactivity with SMO ablation in WT WM at 3 DPL. Scale bar = 25 um.

(H) Quantitative analysis of cells expressing CC1+ oligodendrocytes following SMO ablation. Values are mean + SEM. *p < 0.05, **p < 0.01; two-way ANOVA analysis.

(I) Quantitative analysis of changes in NG2+ cells following SMO ablation. Values are mean + SEM. *p < 0.05, **p < 0.01; two-way ANOVA analysis.

(J) Confocal images of apoptotic cells expressing Cleaved caspase-3 (red) in WT and CNPSox17 mice after SMO ablation at 3 DPL. Scale bar = 20 um.

(K) Quantitative analysis of Cl. Caspase-3 + cells in intact (Sal) and lesioned (Lys) WM at 3 DPL. SMO-expressing control groups are indicated by SMO+, and PDGFRCre-targeted SMO-ablated mutants are indicated by SMOf/f. Values are mean + SEM. *p < 0.05, **p < 0.01; two-way ANOVA analysis.

(L) Confocal images of cells expressing Cleaved caspase-3 (red) in WT and CNPSox17 mice following stereotaxic injection of 5 uM cyclopamine (Cyc) in Lys lesions at 3 DPL. Scale bar = 20 um.

(M) Quantitative analysis of the effects of Cyc on demyelination-induced cell death in WT and CNPSox17 mice. Cell density values are mean ± SEM obtained from 3 independent experiments. *p < 0.05, **p < 0.01; two-way ANOVA analysis.

observations support a fundamental role for Hedgehog/Smoothened in WM integrity and/or oligodendroglial maintenance. Taken together, these results indicate that Smoothened expression in adult OPCs is necessary for the maintenance and integrity of oligodendroglia, and Smoothened-related mechanisms are obligatory for Sox17-mediated oligodendrogenesis and cell survival.

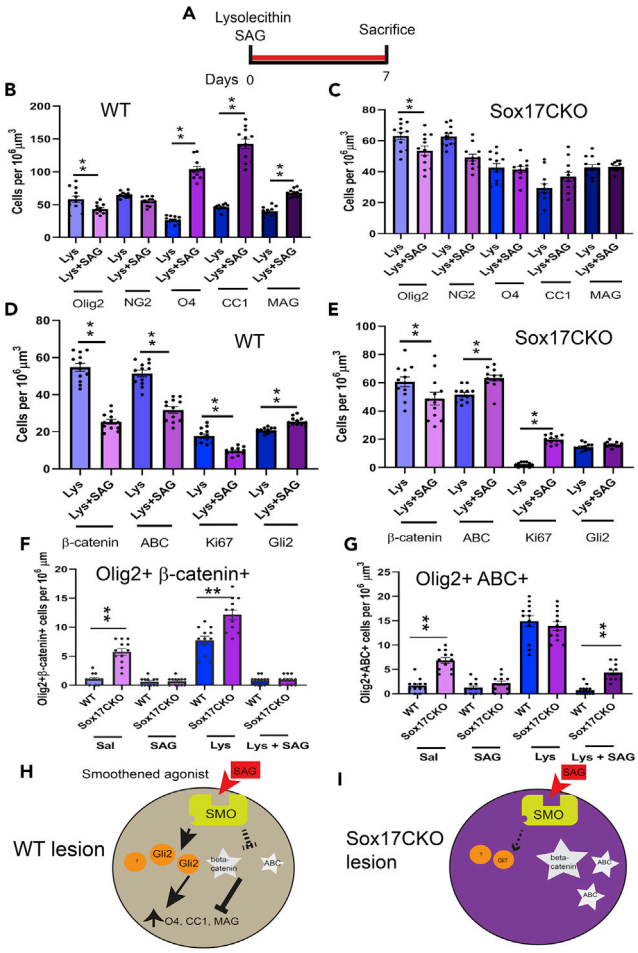


**Figure 7. Oligodendrocyte Regeneration by Smoothened Stimulation Is Dependent on Sox17**

(A) Illustration of stimulation paradigm using 5 uM Smoothened agonist (SAG) with Lysolecithin, followed by analysis at 7 DPL.

(B) Quantitative analysis of effects of SAG on oligodendroglial cell density in WT lesions (Lys). Values are mean + SEM. **p < 0.01; two-way ANOVA.

(C) Quantitative analysis of effects of SAG on oligodendroglial cell density in Sox17CKO lesions (Lys). Values are mean + SEM. **p < 0.01; two-way ANOVA.

(D) Quantitative analysis of effects of SAG on cells expressing beta-catenin, ABC, Ki67, and Gli2 in WT lesions (Lys). Values are mean + SEM. **p < 0.01; two-way ANOVA.

(E) Quantitative analysis of effects of SAG on cells expressing beta-catenin, ABC, Ki67, and Gli2 in Sox17CKO lesions (Lys). Values are mean + SEM. **p < 0.01; two-way ANOVA.

(F) Quantitative analysis of effects of SAG on Olig2 cells that express beta-catenin in intact (SAG) and lesioned (Lys + SAG) WM of WT and Sox17CKO mice. Values are mean + SEM. **p < 0.01; two-way ANOVA.

(G) Quantitative analysis of effects of SAG on Olig2 cells that express ABC in intact (SAG) and lesioned (Lys + SAG) WM of WT and Sox17CKO mice. Cell density values are mean ± SEM obtained from 3 independent experiments. *p < 0.05, **p < 0.01; two-way ANOVA analysis.

(H) Proposed mechanism of SAG action in WT lesions: inducing Gli2 and suppression of ABC, both contributing to increased oligodendroglial differentiation and regeneration.

(I) In Sox17CKO lesions, SAG is unable to induce Gli2, and instead increases beta-catenin while only partially suppressing ABC.

## Smoothened-Induced Beta-Catenin Regulation and OL Regeneration Are Sox17 Dependent

Since Sonic Hedgehog is critical to oligodendrogenesis, we hypothesized that regenerative cell production could be enhanced by direct stimulation of Smoothened activity with a small-molecule agonist, an approach that would circumvent possible deficiencies in endogenous Hedgehog ligand and Patched

co-receptor levels in demyelinating lesions. By using a co-administration paradigm, stereotaxic injection of 5-uM Smoothened agonist (SAG) with lysolecithin in WT controls (Figure 7A, Lys + SAG) increased the formation of O4, CC1, and MAG OLs compared with Lyso alone (Figure 7B, Table S1). Olig2 cells increased with SAG in intact WM of both WT and Sox17CKO (Tables S1 and S2, SAG/Sal; Figure S6A), indicating an oligodendrogenic response to Smoothened activation. However, similar injections in lesions of the Sox17CKO failed to maintain NG2+ cell levels (Figures 7C, S6B, and S6C) or to increase MAG and CC1 OL regeneration (Figure 7C, Table S3, and Figures S6D–S6F), despite a robust NG2+ and CC1 cell response in intact WM (Figures S6B and S6D). The lack of increase in MAG cells with SAG in the intact and lesioned Sox17CKO indicates impairment in OL differentiation (Table S3, CKO/WT). These observations indicate that Smoothened activation may be considered in therapeutic strategies to improve OL regeneration.

The oligodendroglial changes in response to SAG in WT lesions were accompanied by increased Gli2 cells and reduced the total number of cells expressing beta-catenin and ABC (Figure 7D, Table S1). In contrast, WM lesions in the Sox17CKO show no increase in Gli2 cells (Figures 7E, S6G, and S6H, Table S2). There was also a smaller decline in total beta-catenin with SAG, consistent with an impaired response to SAG (Figures 7E, S7A, and S7B, Lys + SAG vs Lys). These support the interpretation that signaling by SAG is dependent on Sox17. The Sox17-dependent defect in Gli2 may account for the failure of cellular regeneration. Dysregulated beta-catenin control likely also contributes to this failure.

Indeed, unlike WT lesions, SAG was unable to suppress total levels of ABC + cells in Sox17CKO lesions (Table S3, Lys + SAG), suggesting altered beta-catenin control by SAG in the absence of Sox17. In contrast, in intact WT tissue, SAG increased total ABC-expressing cells without affecting total beta-catenin levels (Figures S7B and S7D, Sal vs SAG), indicating a function for Smoothened acting upstream of beta-catenin.

To determine whether changes in beta-catenin control could be observed in oligodendroglia, beta-catenin and ABC were analyzed within the Olig2 cell population. As expected, the lesion environment itself increased beta-catenin+ Olig2+ (Figures 7F and S7A) and ABC + Olig2+ (Figures 7G and S7C) cells relative to intact tissue (Sal vs Lys) in both mouse strains. In both WT and Sox17CKO lesions, SAG application suppressed Olig2+ABC+, Olig2+beta-catenin+ (Figures 7F, 7G, S7A, and S7C), and total beta-catenin (Figure S7A). Notably, SAG application in the intact Sox17CKO also suppressed Olig2+beta-catenin+ and Olig2+ABC+ cells in intact Sox17CKO WM (Figures 7F and 7G, Sal vs SAG). The diagrams in Figures 7H and 7I summarize our observations that Smoothened activation with SAG can suppress ABC in WT Olig2+ cells. This is more efficient in WT than in Sox17CKO lesions. In Sox17CKO lesions, despite oligodendroglia-specific suppression of ABC by SAG, cell regeneration did not occur. It is likely that the deficient Gli2 response underlies the failure of cell regeneration. This suggests the requirement for additional Sox17-dependent events that contribute to Gli2 expression and/or activation, efficient ABC suppression, and cell production.

Taken together, these observations indicate that successful oligodendrogenesis and regeneration requires Sox17 functionality for Hedgehog signaling. Our results thus support the interpretation that Sox17 potentiates Hedgehog signaling and its regulation of the Wnt/beta-catenin pathway. These may potentially contribute viable strategies toward amelioration of demyelination pathologies.

## DISCUSSION

Studies of morphogen signaling mechanisms in WM repair have shown that developmental regulation of these pathways critically regulate cell regeneration and recovery from damage. Despite promising outcome following pharmacological Wnt/beta-catenin inhibition in WM lesions (Fancy et al., 2009), this approach to therapy is not without its challenges, given the multitude of developmental processes that involve Wnt-related pathways. Identifying upstream physiological regulators of Wnt may circumvent these challenges. Interestingly, despite an upregulation of Shh by reactive glia in multiple sclerosis WM lesions (Wang et al., 2008), Shh signaling deficiency in WM disease has been described and implicated in the failure of progenitor cell differentiation (Mastronardi et al., 2003; Wang et al., 2008). Interactions between signaling pathways have been described between Shh and Wnt in regulating neurogenesis (Tang et al., 2010) and cortical progenitor cell proliferation in the developing neural tube (Alvarez-Medina et al., 2009). In agreement with these reports, we demonstrate that in the adult WM, Shh, through Smoothened activity, functions upstream to regulate beta-catenin. While Shh drives OL lineage specification and

differentiation early in development (Orentas et al., 1999; Tekki-Kessaris et al., 2001; Wang and Almazan, 2016), we observe that, in the adult, Smoothened has a maintenance role in the oligodendroglial lineage. As neurons are a primary source of Shh (Garcia et al., 2010), the finding that removal of Smoothened in astrocytes results in hypertrophy indicates that Shh signaling is important for neuron-astrocyte communication (Garcia et al., 2010). Since cyclopamine significantly reduces Sox17-mediated cell survival and OPC-targeted ablation of Smoothened dramatically disrupts Olig2- and NG2-cell morphogenesis, we conclude that Hedgehog is obligatory for oligodendroglial maintenance and survival in adult WM, in addition to its importance in the postnatal and adult stem cell niche (Palma et al., 2005). Given that Smoothened expression is necessary for cell viability and maintenance, the interpretation of signaling changes following disruption of Hedgehog components in our studies relies more on the genetic ablation of GLI2 rather than that of Smoothened.

Evidence for neuroprotection by Shh signaling is gaining support: Smoothened agonist purmorphamine is protective in a post-ischemic treatment paradigm, attenuating inflammation and reactive gliosis (Chechneva et al., 2014). In WM, adenoviral Shh expression is known to increase remyelination in lesions through progenitor cell proliferation and differentiation (Ferent et al., 2013). SAG has also recently been shown to improve remyelination after chronic demyelination (Sanchez et al., 2018). In our studies, Sox17 overexpression is characterized by enhanced levels of Shh associated with Olig2 cells and attenuated lysolecithin-induced demyelination damage (Figure 1E) (Ming et al., 2013). It is possible that these properties of the CNPSox17 WM are due in part to both Shh-related survival signaling (e.g., bcl2) (Ming et al., 2013), which may underlie resistance to ultrastructural change with lysolecithin, and Shh-mediated oligodendrogenesis, which facilitates cell replacement.

A functional association between Sox17 and Hedgehog signaling has not previously been reported in CNS. Sox18, another member of the SoxF family, was reported to be a target gene of Hedgehog/GLI in cervical carcinoma cells. Unlike Sox17, Sox18 did not influence cell proliferation, but instead migration and invasion (Petrovic et al., 2015). Control of Hedgehog signaling is complex because regulation occurs at multiple molecular levels (Falkenstein and Vokes, 2014). The enhanced immunoreactivity of Shh localized with Olig2 as a result of Sox17 overexpression suggests differential sequestration and/or preservation of membrane integrity. Our observation that SAG fails to stimulate oligodendrogenesis in the Sox17CKO suggests additional contribution by alteration in the cellular response to Smoothened activation. Sox17 could contribute to stabilization and enhancement of Gli2 levels through Sox17-induced Notch signaling (Chew et al., 2019). Notch has been shown to function upstream as a signaling hub with Shh, and Notch inhibition results in reduced Gli mediator activity (Ravanelli et al., 2018; Yabut et al., 2015). Notch signaling regulates the Shh receptor Patched1 and enables cells to interpret Shh gradients for cell fate determination (Kong et al., 2015). Since we observed impaired Gli2 induction by SAG in Sox17CKO, we think it is possible that either Smoothened/Patched function is impaired or Gli2 levels are reduced as an indirect result of Notch deficiency (Ringuette et al., 2016).

The mechanisms by which Hedgehog mediators impact beta-catenin are not well understood. Gli repressor forms, particularly Gli3R, are known to inhibit canonical Wnt signaling by direct interaction with beta-catenin (Ulloa et al., 2007). Shh antagonism of Wnt (Ding and Wang, 2017) may additionally be contributed by SFRP (He et al., 2006; Katoh and Katoh, 2006), a regulated target of Sox17 (Chew et al., 2011). SFRP1 regulation of Wnt3a (Galli et al., 2006) or GSK3beta activity (Peng et al., 2019) in turn alters beta-catenin localization and function (Peng et al., 2019). The precise mechanisms that regulate Notch, Shh, and Wnt activity are highly context-specific; therefore, the events by which changes in Hedgehog signaling determines beta-catenin regulation remain to be fully elucidated.

Sox proteins are known to antagonize beta-catenin (Chew and Gallo, 2009); however, it is surprising that in adult WM, unlike in developing WM (Chew et al., 2011), Sox17-mediated regulation of beta-catenin did not involve direct binding between Sox17 and beta-catenin. An increased involvement of Hedgehog signaling in adult WM is consistent with the recent observation that Shh expression in the early postnatal brain is undetectable, but rises by P14 (Rivell et al., 2019), coincident with active developmental myelination. Similar to Sox9 in chondrocytes (Topol et al., 2009), Sox17 overexpression was found to increase beta-catenin phosphorylation in adult WM, reducing unphosphorylated, stabilized beta-catenin. In other systems, Sox17 also regulates muscle satellite cell expansion and renewal by inhibiting beta-catenin activity (Alonso-Martin et al., 2018). Strikingly, both beta-catenin and ABC in Olig2 cells were suppressed by SAG in Sox17CKO (Figures 7F and 7G), indicating that Sox17-expressing oligodendroglia rely on Smoothened to regulate beta-catenin abundance and activity

through the same pathway. The finding that total ABC-expressing cells were not suppressed by SAG in Sox17-deficient lesions reveals a cell-specific, Sox17-dependent component of ABC control. Given that Notch signaling has been reported to regulate Wnt/beta-catenin (Li et al., 2016; Tian et al., 2015), other possible mechanisms involving Hedgehog signaling modulation by Sox17 await future investigation.

Taken together, our studies reveal a previously uncharacterized functional relationship between Sox17 and Hedgehog signaling and provide clues to how Sox transcription factors regulate oligodendroglial cell regeneration in the CNS. Hedgehog signaling is dependent on Sox17, and the integration of Hedgehog with Wnt/beta-catenin is dynamically regulated in oligodendroglia. Sox17-mediated Hedgehog signaling and its modulation of Hedgehog-Wnt interaction in WM lesions contributes to the progenitor cell response in tissue repair. Future regenerative therapies may therefore benefit from the stimulation of Sox17 targets in demyelinating pathologies.

### Limitations of the Study

This study was largely conducted in *in vivo* model systems. While we have presented evidence for Sox17 regulation of Hedgehog, the mechanism by which Sox17 or its target gene Notch1 affects Hedgehog responsiveness is not known in oligodendroglia and is a subject for future research. Further molecular studies may be performed in culture systems, but the control of morphogen signals *in vitro* is subject to experimental variables that do not readily reconstitute conditions in isolated oligodendroglia similar to those present in adult acutely remyelinating WM.

### Resource Availability

#### *Lead Contact*

Further information and requests should be directed to and will be fulfilled by the Lead Contact, Vittorio Gallo (vgallo@childrensnational.org).

#### *Materials Availability*

At the time of re-submission, neither the CNPSox17 mouse line nor Sox17 floxed allele has been deposited with an external centralized repository for its distribution. Therefore, these lines are available for sharing from the Lead Contact with a completed Materials Transfer Agreement.

#### *Data and Code Availability*

This study did not generate any unique data sets or code.

## METHODS

All methods can be found in the accompanying Transparent Methods supplemental file.

## SUPPLEMENTAL INFORMATION

Supplemental Information can be found online at https://doi.org/10.1016/j.isci.2020.101592.

## ACKNOWLEDGMENTS

We thank Drs. Jyoti Jaiswal and Shivaprasad Bhuvanendran for advice on cellular imaging and data analysis. This work was supported by the National Multiple Sclerosis Society RG4706A4/2 and RR-1512-07066 (V.G.) and partially supported by FISM 2015/R/13 (V.G.) and VA I01BX002565-05 (J.D.). Confocal and fluorescence microscopy portions of this project were performed in the Neuroimaging Core, supported by award number 1U54HD090257 from the NIH, District of Columbia Intellectual and Developmental Disabilities Research Center Award (DC-IDDRDC, VG). The contents of this work are solely the responsibility of the authors and do not represent the official views of the DC-IDDRC or NIH.

## AUTHOR CONTRIBUTIONS

L-.J.C. and V.G. conceptualized the study. X.T.M. and L-.J.C. maintained mouse colonies and designed the experiments. X.T.M. performed the majority of the experiments, and L-.J.C. performed immunohistochemical analyses and Western blots and conducted reporter assays. J.D. prepared brain samples and generated EM images. X.T.M. and L-.J.C. performed data analysis and prepared the figures. X.T.M., L-.J.C., and V.G. wrote the paper. L-.J.C. and V.G. obtained funding, and V.G. and L-.J.C. coordinated the project.

## DECLARATION OF INTERESTS

X.M., L-J.C., J.D., and V.G. declare no competing interests.

Received: April 13, 2020
Revised: August 29, 2020
Accepted: September 16, 2020
Published: October 23, 2020

## REFERENCES

Alonso-Martin, S., Aurade, F., Mademtzoglou, D., Rochat, A., Zammit, P.S., and Relaix, F. (2018). SOXF factors regulate murine satellite cell self-renewal and function through inhibition of beta-catenin activity. Elife *7*, pii: e26039.

Alvarez-Medina, R., Le Dreau, G., Ros, M., and Marti, E. (2009). Hedgehog activation is required upstream of Wnt signalling to control neural progenitor proliferation. Development *136*, 3301–3309.

Chechneva, O.V., Mayrhofer, F., Daugherty, D.J., Krishnamurty, R.G., Bannerman, P., Pleasure, D.E., and Deng, W. (2014). A Smoothened receptor agonist is neuroprotective and promotes regeneration after ischemic brain injury. Cell Death Dis. *5*, e148.

Chew, L., Ming, X., McEllin, B., Dupree, J., Hong, E., Catron, M., Fauveau, M., Nait-Oumesmar, B., and Gallo, V. (2019). Sox17 regulates a program of oligodendrocyte progenitor cell expansion and differentiation during development and repair. Cell Rep. *29*, 3173–3186.

Chew, L.J., and Gallo, V. (2009). The Yin and Yang of Sox proteins: activation and repression in development and disease. J. Neurosci. Res. *87*, 3277–3287.

Chew, L.J., Shen, W., Ming, X., Senatorov, V.V.J., Chen, H.-L., Cheng, Y., Hong, E., Knoblach, S., and Gallo, V. (2011). SRY-box containing gene 17 regulates the Wnt/beta-catenin signaling pathway in oligodendrocyte progenitor cells. J. Neurosci. *31*, 13921–13935.

Dimou, L., and Gallo, V. (2015). NG2-Glia and their functions in the central nervous system. GLIA *63*, 1429–1451.

Ding, M., and Wang, X. (2017). Antagonism between Hedgehog and Wnt signaling pathways regulates tumorigenicity (Review). Oncol. Lett. *14*, 6327–6333.

Falkenstein, K.N., and Vokes, S.A. (2014). Transcriptional regulation of graded hedgehog signaling. Semin. Cell Dev. Biol. *33*, 73–80.

Fan, R., He, H., Yao, W., Zhu, Y., Zhou, X., Gui, M., Lu, J., Xi, H., Deng, Z., and Fan, M. (2018). SOX7 suppresses Wnt signaling by disrupting beta-catenin/BCL9 interaction. DNA Cell Biol. *37*, 126–132.

Fancy, S.P., Harrington, E.P., Baranzini, S.E., Silbereis, J.C., Shiow, L.R., Yuen, T.J., Huang, E.J., Lomvardas, and Rowitch, D. (2014). Parallel states of pathological Wnt signaling in neonatal brain injury and colon cancer. Nat. Neurosci. *17*, 506–512.

Fancy, S.P.J., Baranzini, S.E., Zhao, C., Yuk, D.-I., Irvine, K.-A., Kaing, S., Sanai, N., Franklin, R.J.M., and Rowitch, D.H. (2009). Dysregulation of the Wnt pathway inhibits timely myelination and remyelination in the mammalian CNS. Genes Dev. *23*, 1571–1585.

Ferent, J., Zimmer, C., Durbec, P., Ruat, M., and Traiffort, E. (2013). Sonic hedgehog signaling is a positive oligodendrocyte regulator during demyelination. J. Neurosci. *33*, 1759–1772.

Fu, D.-Y., Wang, Z.-M., Chen, L., Wang, B.-L., Shen, Z.-Z., Huang, W., and Shao, Z.-M. (2010). Sox17, the canonical Wnt antagonist, is epigenetically inactivated by promoter methylation in human breast cancer. Breast Cancer Res. Treat. *119*, 601–612.

Galli, L.M., Barnes, T.R., Cheng, T., Acosta, L., Anglade, A., Willert, K., Nusse, R., and Burrus, L.W. (2006). Differential inhibition of Wnt-3a by Sfrp-1, Sfrp-2, and Sfrp-3. Dev. Dyn. *235*, 681–690.

Garcia, A.D.R., Petrova, R., Eng, L., and Joyner, A.L. (2010). Sonic Hedgehog regulates discrete populations of astrocytes in the adult mouse forebrain. J. Neurosci. *30*, 13597–13608.

Guo, F., Lang, J., Sohn, J., Hammond, E., Chang, M., and Pleasure, D. (2015). Canonical Wnt signaling in the oligodendroglial lineage - puzzles remain. Glia *63*, 1671–1693.

He, J., Sheng, T., Stelter, A.A., Li, C., Zhang, X., Sinha, M., Luxon, B.A., and Xie, J. (2006). Suppressing Wnt signaling by the hedgehog pathway through sFRP1. J. Biol. Chem. *281*, 35598–35602.

Jia, Y., Yang, Y., Liu, S., Herman, J.G., Lu, F., and Guo, M. (2010). Sox17 antagonizes WNT/beta-catenin signaling pathway in hepatocellular carcinoma. Epigenetics *5*, 743–749.

Katoh, Y., and Katoh, M. (2006). WNT antagonist, SFRP1, is Hedgehog signaling target. Int. J. Mol. Med. *17*, 171–175.

Kong, J.H., Yang, L., Dessaud, E., Chuang, K., Moore, D.M., Rohatgi, R., Briscoe, J., and Novitch, B.G. (2015). Notch activity modulates the responsiveness of neural progenitors to sonic hedgehog signaling. Dev. Cell *33*, 373–387.

Langseth, A.J., Munji, R.N., Choe, Y., Huynh, T., Pozniak, C.D., and Pleasure, S.J. (2010). Wnts influence the timing and efficiency of oligodendrocyte precursor cell generation in the telencephalon. J. Neurosci. *30*, 13367–13372.

Li, C.-T., Liu, J.-X., Yu, B., Liu, R., Dong, C., and Li, S.-J. (2016). Notch signaling represses hypoxia-inducible factor-1a-induced activation of Wnt/b-catenin signaling in osteoblasts under cobalt-mimicked hypoxia. Mol. Med. Rep. *14*, 689–696.

Mastronardi, F.G., daCruz, L.A., Wang, H., Boggs, J., and Moscarello, M.A. (2003). The amount of sonic hedgehog in multiple sclerosis white matter is decreased and cleavage to the signaling peptide is deficient. Mult. Scler. *9*, 362–371.

Merchan, P., Bribian, A., Sanchez-Camacho, C., Lezameta, M., Bovolenta, P., and De Castro, F. (2007). Sonic hedgehog promotes the migration and proliferation of optic nerve oligodendrocyte precursors. Mol. Cell Neurosci. *36*, 355–368.

Ming, X., Chew, L.J., and Gallo, V. (2013). Transgenic overexpression of Sox17 promotes oligodendrocyte development and attenuates demyelination. J. Neurosci. *33*, 12528–12542.

Moll, N.M., Hong, E., Fauveau, M., Naruse, M., Kerninon, C., Tepavcevic, V., Klopstein, A., Seilhean, D., Chew, L.J., Gallo, V., et al. (2013). Sox17 is expressed in regenerating oligodendrocytes in experimental models of demyelination and in multiple sclerosis. Glia *61*, 1659–1672.

Nery, S., Wichterle, H., and Fishell, G. (2001). Sonic hedgehog contributes to oligodendrocyte specification in the mammalian forebrain. Development *128*, 527–540.

Nicolay, D.J., Doucette, J.R., and Nazarali, A.J. (2007). Transcriptional control of oligodendrogenesis. Glia *55*, 1287–1299.

Orentas, D.M., Hayes, J.E., Dyer, K.L., and Miller, R.H. (1999). Sonic Hedgehog signaling is required during the appearance of spinal cord oligodendrocyte precursors. Development *126*, 2419–2429.

Palma, V., Lim, D.A., Dahmane, N., Sanchez, P.J., Brionne, T.C., Herzberg, C.D., Gitton, Y., Carleton, A., Alvarez-Buylla, A., and Ruiz i Altaba, A. (2005). Sonic hedgehog controls stem cell behavior in the postnatal and adult brain. Development *132*, 335–344.

Peng, J.-X., Llang, S.-Y., and Li, L. (2019). sFRP1 exerts effects on gastric cancer cells through GSK3b/Rac1-mediated restraint of TGFb/Smad3 signaling. Oncol. Rep. *41*, 224–234.

Petrovic, I., Milivojevic, M., Popovic, J., Schwirtlich, M., Rankovic, B., and Stevanovic, M. (2015). Sox18 is a novel target gene of hedgehog signaling in cervical carcinoma cell lines. PLoS One *10*, e0143591.

Potzner, M.R., Griffel, C., Lutjen-Drecoll, E., Bosl, M.R., Wegner, M., and Sock, E. (2007). Prolonged Sox4 expression in oligodendrocytes interferes

with normal myelination in the central nervous system. Mol. Cell. Biol. *27*, 5316–5326.

Ravanelli, A.M., Kearns, C.A., Powers, R.K., Wang, Y., Hines, J.H., Donaldson, M.J., and Appel, B. (2018). Sequential specification of oligodendrocyte lineage cells by distinct levels of hedgehog and notch signaling. Dev. Biol. *444*, 93–106.

Ringuette, R., Atkins, M., Lagali, P.S., Bassett, E.A., Campbell, C., Mazerolle, C., Mears, A.J., Picketts, D.J., and Wallace, V.A. (2016). A Notch-Gli2 axis sustains Hedgehog responsiveness of neural progenitors and Muller glia. Dev. Biol. *411*, 85–100.

Rivell, A., Petralia, R.S., Wang, Y.-X., Clawson, E., Moehl, K., Mattson, M.P., and Yao, P.J. (2019). Sonic hedgehog expression in the postnatal brain. Biol. Open *8*, bio040592.

Rowitch, D.H., St.-Jacques, B., Lee, S.M.K., Flax, J.D., Snyder, E.Y., and McMahon, A.P. (1999). Sonic hedgehog regulates proliferation and inhibits differentiation of CNS precursor cells. J. Neurosci. *19*, 8954–8965.

Samanta, J., Grund, E.M., Silva, H.M., Safaille, J.J., Fishell, G., and Salzer, J.L. (2015). Inhibition of Gli1 mobilizes endogenous neural stem cells for remyelination. Nature *526*, 448–452.

Sanchez, M.A., and Armstrong, R.C. (2018). Postnatal Sonic Hedgehog (SHH) responsive cells give rise to oligodendrocyte lineage cells during myelination and in adulthood contribute to remyelination. Exp. Neurol. *299*, 122–136.

Sanchez, M.A., Sullivan, G.M., and Armstrong, R.C. (2018). Genetic detection of Sonic hedgehog (Shh) expression and cellular response in the progression of acute through chronic demyelination and remyelination. Neurobiol. Dis. *115*, 145–156.

Sohn, J., Natale, J.E., Chew, L.J., Belachew, S., Cheng, Y., Aguirre, A.A., Lytle, J., Nait-Oumesmar, B., Kerninon, C., Kanai-Azuma, M., et al. (2006). Identification of Sox17 as a transcription factor that regulates oligodendrocyte development. J. Neurosci. *26*, 9722–9735.

Stolt, C.C., Lommes, P., Sock, E., Chaboissier, M.C., Schedl, A., and Wegner, M. (2003). The Sox9 transcription factor determines glial fate choice in the developing spinal cord. Genes Dev. *17*, 1677–1689.

Stolt, C.C., Rehberg, S., Ader, M., Lommes, P., Riethmacher, D., Schachner, M., Bartsch, U., and Wegner, M. (2002). Terminal differentiation of myelin-forming oligodendrocytes depends on the transcription factor Sox10. Genes Dev. *16*, 165–170.

Takezaki, T., Hide, T., Takanaga, H., Nakamura, H., Kuratsu, J., and Kondo, T. (2011). Essential role of the Hedgehog signaling pathway in human glioma-initiating cells. Cancer Sci. *102*, 1306–1312.

Tang, M., Villaescusa, J.C., Luo, S.X., Guitarte, C., Lei, S., Miyamoto, Y., Taketo, M.M., Arenas, E., and Huang, E.J. (2010). Interactions of Wnt/beta-catenin signaling and Sonic Hedgehog regulate the neurogenesis of Ventral midbrain dopaminergic neurons. J. Neurosci. *30*, 9280–9291.

Tekki-Kessaris, N., Woodruff, R., Hall, A.C., Gaffield, W., Kimura, S., Stiles, C.D., Rowitch, D.H., and Richardson, W.D. (2001). Hedgehog-dependent oligodendrocyte lineage specification in the telencephalon. Development *128*, 2545–2554.

Tian, H., Biehs, B., Chiu, C., Siebel, C.W., Wu, Y., Costa, M., De Sauvage, F.J., and Klein, O.D. (2015). Opposing activities of Notch and Wnt signaling regulate intestinal stem cells and Gut Homeostasis. Cell Rep. *11*, 33–42.

Topol, L., Chen, W., Song, H.S., Day, T.F., and Yang, Y.J. (2009). Sox9 inhibits Wnt signaling by promoting beta-catenin phosphorylation in the nucleus. J. Biol. Chem. *284*, 3323–3333.

Ulloa, F., Itasaki, N., and Briscoe, J. (2007). Inhibitory Gli3 activity negatively regulates Wnt/b-catenin signaling. Curr. Biol. *17*, 545–550.

Wang, L.-C., and Almazan, G. (2016). Role of Sonic Hedgehog signaling in oligodendrocyte differentiation. Neurochem. Res. *41*, 3289–3299.

Wang, Y., Imitola, J., Rasmussen, S., O'Connor, K.C., and Khoury, S.J. (2008). Paradoxical dysregulation of the neural stem cell pathway Sonic hedgehog-Gli1 in autoimmune encephalomyelitis and multiple sclerosis. Ann. Neurol. *64*, 417–427.

Yabut, O., Pleasure, S.J., and Yoon, K. (2015). A notch above sonic hedgehog. Dev. Cell *33*, 371–372.

Yeung, M.S.Y., Djelloul, M., Steiner, E., Bernard, S., Salehpour, M., Possnert, G., Brundin, L., and Frisen, J. (2019). Dynamics of oligodendrocyte generation in multiple sclerosis. Nature *566*, 538–542.

Yuan, X., Chittajallu, R., Belachew, S., Anderson, S., McBain, C.J., and Gallo, V. (2002). Expression of the green fluorescent protein in the oligodendrocyte lineage: a transgenic mouse for developmental and physiological studies. J. Neurosci. Res. *70*, 529–545.

Zorn, A.M., Barish, G.D., Williams, B.O., Lavender, P., Klymkowsky, M.W., and Varmus, H.E. (1999). Regulation of Wnt signaling by Sox proteins: XSox17 alpha/beta and XSox3 physically interact with beta-catenin. Mol. Cell *4*, 487–498.

**iScience, Volume *23***

## Supplemental Information

# Sox17 Promotes Oligodendrocyte Regeneration by Dual Modulation of Hedgehog and Wnt Signaling

**Xiaotian Ming, Jeffrey L. Dupree, Vittorio Gallo, and Li-Jin Chew**

Supplementary Figure 1

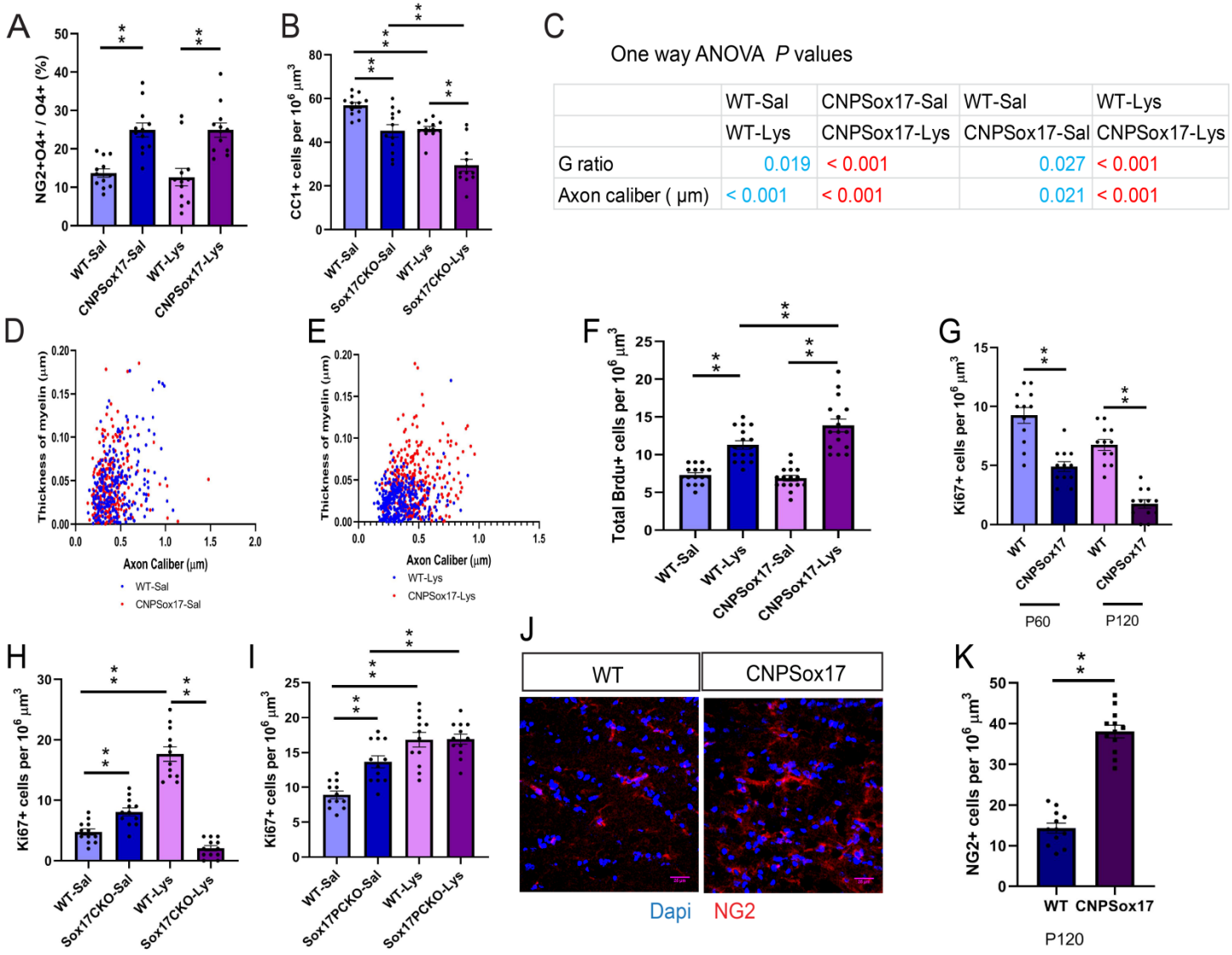


| | WT-Sal | CNPSox17-Sal | WT-Sal | WT-Lys |
|---|---|---|---|---|
| | WT-Lys | CNPSox17-Lys | CNPSox17-Sal | CNPSox17-Lys |
| G ratio | 0.019 | < 0.001 | 0.027 | < 0.001 |
| Axon caliber ( µm) | < 0.001 | < 0.001 | 0.021 | < 0.001 |

**Supplementary Figure 1. Analysis of myelin lesions in Sox17 mutants at P60, unless otherwise indicated. Related to Figure 1 and Figure 2.** (A) Quantitative analysis showing increased percentage of dual-labeled NG2+O4+ cells in CNPSox17 WM. (B) Quantitative analysis showing decreased CC1+ cells in Sox17CKO lesions at 7DPL. (C) Table of One-way ANOVA *P* values to indicate significant changes in G ratio and Axon caliber of measurements shown in Figure 1G and Figure 1H. Values in red indicate increases, and blue indicate decreases. (D) Myelin thickness measurements in intact (Sal) WT and CNPSox17 WM. (E) Myelin thickness in lesions (Lys) of WT and CNPSox17 WM. (F) Quantitative analysis showing increased nascent BrdU+ labeled cells in CNPSox17 lesions. (G) Quantitative analysis showing decreased Ki67+ proliferative cells in intact (Sal) CNPSox17 tissue at 7 DPL (H) Quantitative analysis showing increased Ki67+ cells in intact (Sal) Sox17CKO tissue at 7DPL. (I) Quantitative analysis showing elevated Ki67+ cells in intact (Sal) Sox17PCKO tissue at 7 DPL. Cell density values are mean and SEM obtained from 3 independent experiments.*P <0.05, ** P <0.01; two way ANOVA analysis. (J) Confocal microscope images showing NG2-expressing cells (red) in intact P120 WT and CNPSox17 WM. Scale bar = 25 um. (K) Quantitative analysis showing significant increase in NG2+ cells in CNPSox17 WM at P120. Cell density values are mean and SEM obtained from 3 independent experiments. Unpaired Student's T-test, ***P*<0.001 vs WT.

Supplementary Figure 2

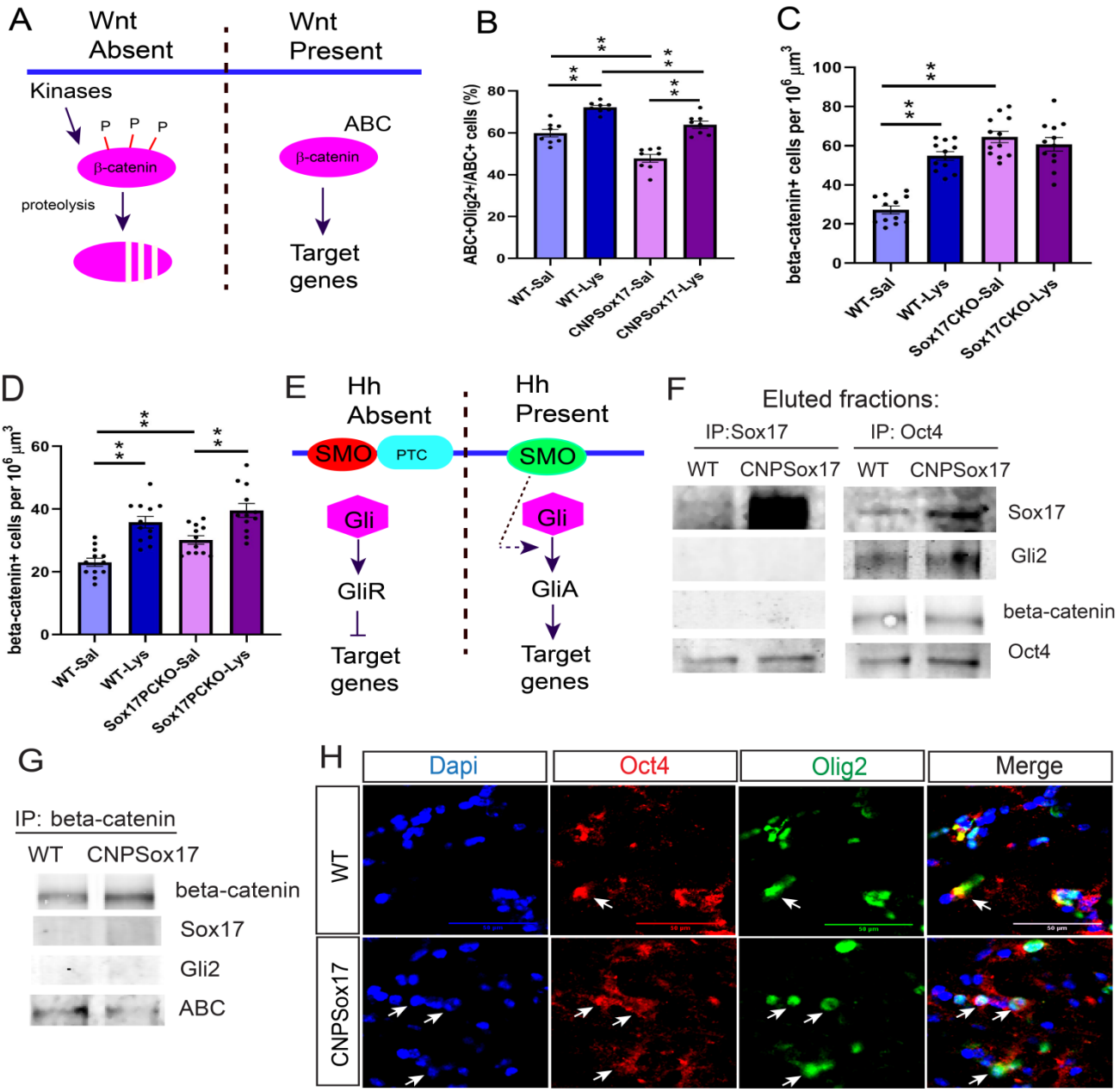


**Supplementary Figure 2. Sox17 regulates beta-catenin and ABC. Related to Figure 3 and Figure 4.** (A) Diagram illustrating cellular conditions without Wnt, generating phosphorylated beta-catenin, leading to its proteolysis or stabilization of unphosphorylated/Active beta-catenin (ABC) with Wnt. (B) The percentage of ABC+ cells belonging to the oligodendroglial lineage is not affected by Sox17 overexpression in CNPSox17. (C) Quantitative analysis showing beta-catenin+ cells are elevated in adult Sox17CKO at 7 DPL. (D) Quantitative analysis showing beta-catenin+ cells are elevated in adult Sox17PCKO at 7DPL. Cell density values are mean and SEM obtained from 3 independent experiments. * P <0.05, ** P <0.01; two way ANOVA analysis. (E) Canonical Hedgehog (Hh) signaling is mediated by ligand-induced release of Smoothened(SMO) from Patched(Ptc). Activated SMO stimulates Gli-activation (GliA) and transcription of target genes (e.g. Gli1). (F) Immunoprecipitation-Western blot assays using tissue lysates from adult WM of WT of CNPSox17 tissue, showing association between Sox17 and Oct4 but not directly between Sox17 and beta-catenin. IP: Immunoprecipitating antibody. (G) Immunoprecipitation assay showing reduced fraction of total immunoprecipitated beta-catenin that consists of active beta-catenin (ABC) in CNPSox17 lysates. (H) Immunocytochemistry of WM showing some colocalization between Oct4(red) and Olig2(green), indicating the expression of Oct4 in some Olig2 cells. Scale bars= 50um.

Supplementary Figure 3

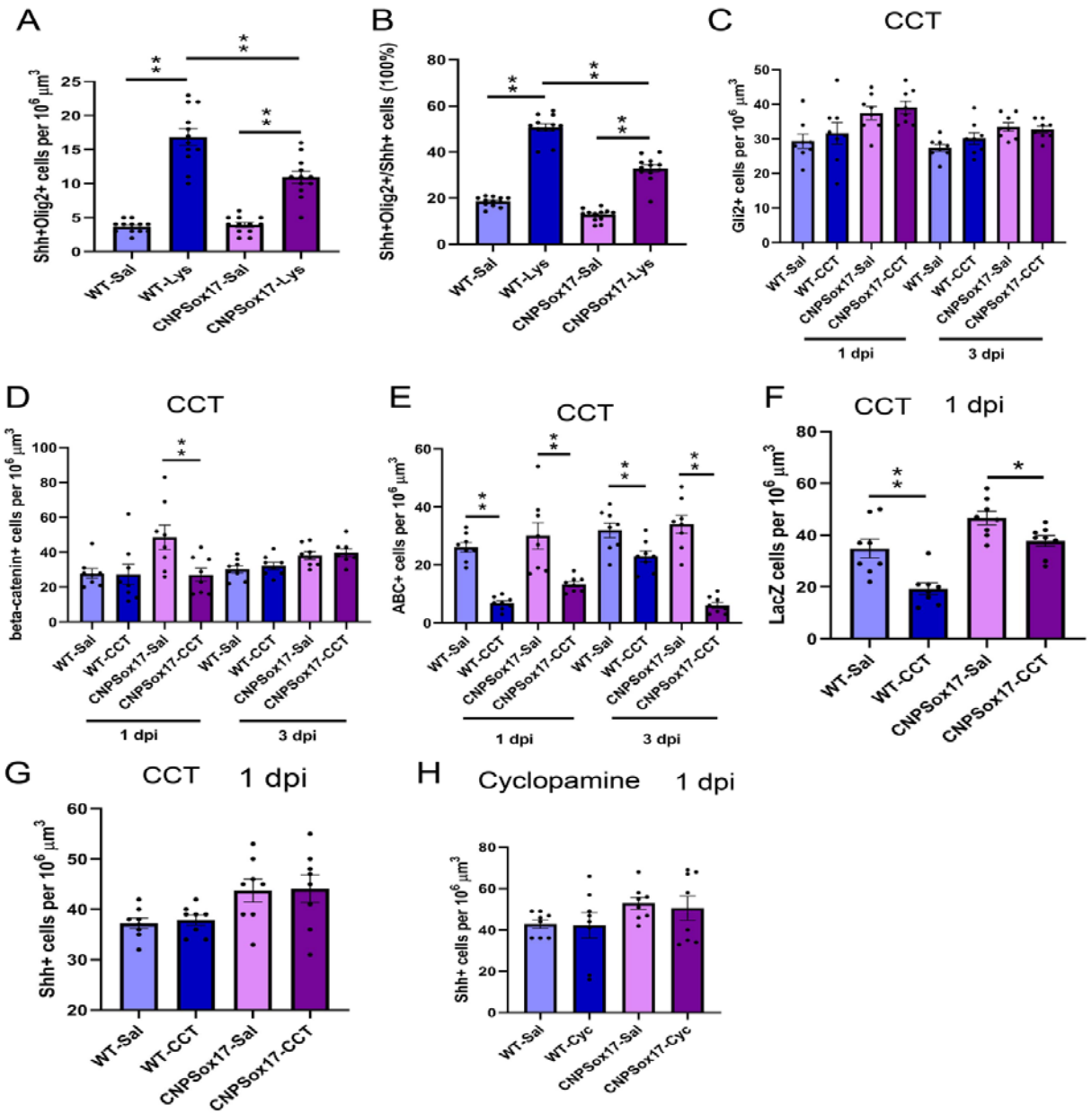


**Supplementary Figure 3**. **Hedgehog inhibitor and beta-catenin inhibitor reveal signaling crosstalk and hierarchy. Related to Figure 4.** (A) Density of Shh+Olig2+ cells is increased in lesions of both strains. (B) Percentage of Shh+ cells that also express Olig2 is increased in lesions of both strains at 3 DPL. (C) Quantitative analysis of beta-catenin+ cells in WT and CNPSox17 WM at 1 and 3 days post injection (dpi) after stereotaxic injection with 2ul 10 uM CCT036477(CCT) into subcortical WM, showing no significant change in Gli2+ cells. (C) Quantitative analysis of Gli2+ cells in WT and CNPSox17 WM at 1 and 3 dpi after stereotaxic injection with 2ul 10 uM CCT into subcortical WM, showing no change in Gli2+ cells with CCT. (D) Quantitative analysis of beta-catenin+ cells in WT and CNPSox17 WM at 1 and 3 dpi, showing that only CNPSox17 responds by decreasing beta-catenin+ cells. (E) Quantitative analysis showing that ABC+ cells are decreased with CCT. (F) Quantitative analysis of LacZ+ cells in WT BATGAL and CNPSox17;BATGAL WM at 1 dpi showing that LacZ+ cells are decreased with CCT. (G) Quantitative analysis of Shh+ cells in WT and CNPSox17 WM at 1 dpi showing no effect of CCT. (F) Quantitative analysis of Shh+ cells in WT and CNPSox17 WM at 1 dpi, showing no effect of 2ul 5uM Cyclopamine. Statistical comparisons were made with two way ANOVA, **P*<0.05, ***P*<0.01.

Supplementary Figure 4

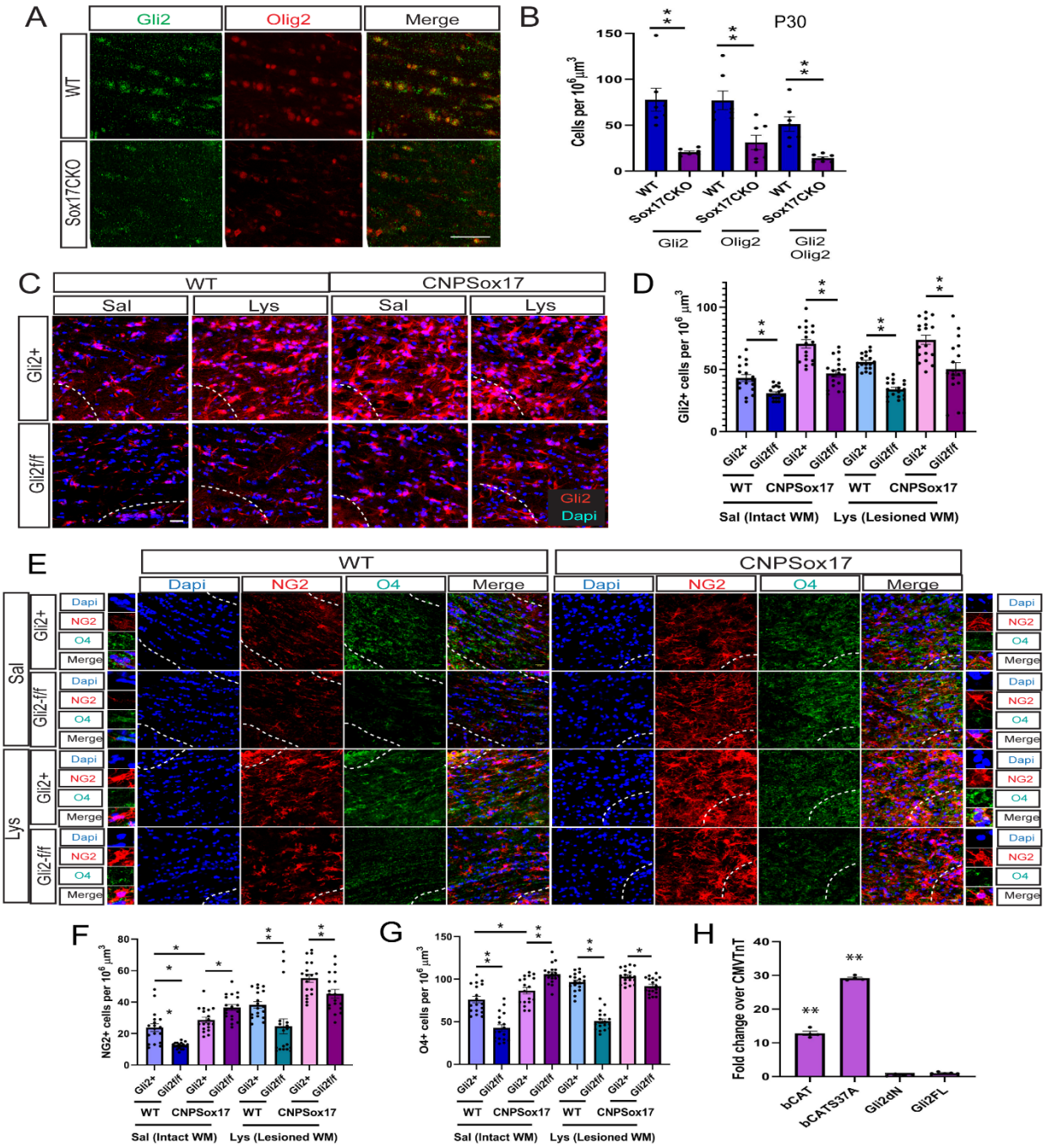


**Supplementary Figure 4. Gli2 mediates Sox17-induced oligodendrogenesis. Related to Figure 5.** (A) Confocal microscope images showing Gli2(green), Olig2(red) and doubly labeled cells (yellow) in P30 WT and Sox17CKO WM. Scale bar = 50 um. (B) Quantitative analysis of Gli2+, Olig2+ and doubly labeled cells at P30. (C) Confocal images of Gli2 (red) cells following Gli2 ablation in WT and CNPSox17 WM in intact (Sal) and lesioned (Lys) WT and CNPSox17 WM. Scale bars=20um. (D) Quantitative changes in Gli2+ cells at 3 DPL following tamoxifen-induced Gli2 ablation. (E) Confocal microscope images of NG2 (red), O4(green) cells following Gli2 ablation in PDGFRaCre;Gli2ff(WT) or PDGFRaCre;Gli2ff;CNPSox17 (CNPSox17) WM in intact (Sal) and lesioned (Lys) WT and CNPSox17 WM at 3DPL. Scale bar=20 um. Dashed lines delineate WM regions adjacent to injection site. (F) Quantitative analysis of cells expressing NG2 following Gli2 ablation. (G) Quantitative analysis of cells expressing O4 following Gli2 ablation. * P <0.05, ** P <0.01; two way ANOVA analysis. (H) In vitro luciferase reporter assays in HEK293 cells to determine transcriptional activity of the indicated expression plasmids at TOPFLASH and FOPFLASH reporters. Relative activity is expressed as fold change of TOPFLASH/FOPFLASH ratios over basal TOPFLASH/FOPFLASH ratio for cotransfected CMVTnT empty vector. Values are mean ± SEM. N=4 experiments. Only Gli2dN and Gli2FL are not significantly different from each other, and are similar to basal activity. One-way ANOVA, Holm-Sidak posthoc test. ***P*<0.01.

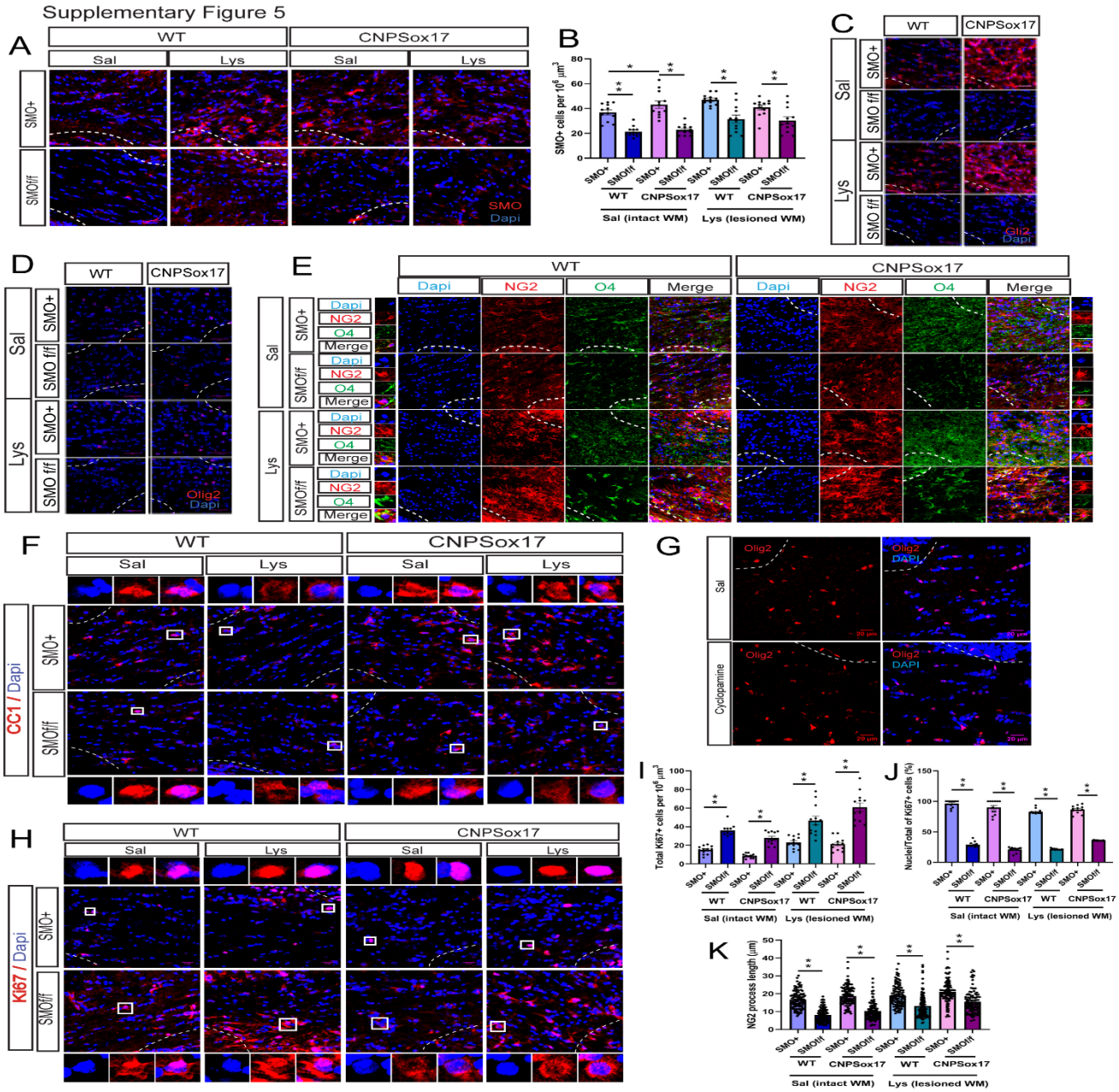


**Supplementary Figure 5. SMO ablation regulates oligodendroglial cells in intact or lesioned WM. Related to Figure 6.** (A) Confocal microscope images of SMO+ cells (red) following ablation in PDGFRaCre;SMOff (WT) or PDGFRaCre;SMOff;CNPSox17 (CNPSox17) mice at 3 DPL. The Tamoxifen paradigm is illustrated in Figure 6. Scale bar= 20 um. Dashed lines delineate WM regions adjacent to injection site. (B) Quantitative analysis of SMO+ cells (red). Cell density values are mean and SEM obtained from 3 independent litters. *$P$<0.05, **$P$ <0.01; two way ANOVA analysis. (C) Confocal images of Gli2+ cells (red) following SMO ablation in intact WT and CNPSox17 WM at 3 DPL. Scale bar=20um. (D) Confocal images of Olig2+ cells (red) following SMO ablation. Scale bar=50um. (E) Confocal images of NG2+ (red) and O4+ (green) cells following SMO ablation at 3 DPL. Scale bar= 20 um. (F) Confocal microscope images showing CC1 cells (red) in intact or lesioned WM following SMO ablation in PDGFRaCre;SMOff (WT) or PDGFRaCre;SMOff;CNPSox17 (CNPSox17) mice at 3 DPL. Scale bar=20um. Cells in boxes are enlarged as individual fluorescent channels above composite panels. (G) Confocal images showing reduced Olig2 immunoreactivity (red) in WT WM 24 h following focal administration of 5 uM Cyclopamine. (H) Confocal images of Ki67+ cells (red) following SMO ablation at 3 DPL. Scale bar=20um. Dashed lines delineate WM regions adjacent to injection site. (I) Quantitative analysis of total Ki67+ cells following SMO ablation at 3 DPL. (J) Analysis of the proportion of Ki67+ cells with nuclear Ki67+ distribution following SMO ablation.(K) Histograms showing decreased NG2 process length in cells lacking SMO. Cell density values are mean and SEM obtained from 3 independent experiments. * P <0.05, ** P <0.01; two way ANOVA analysis.

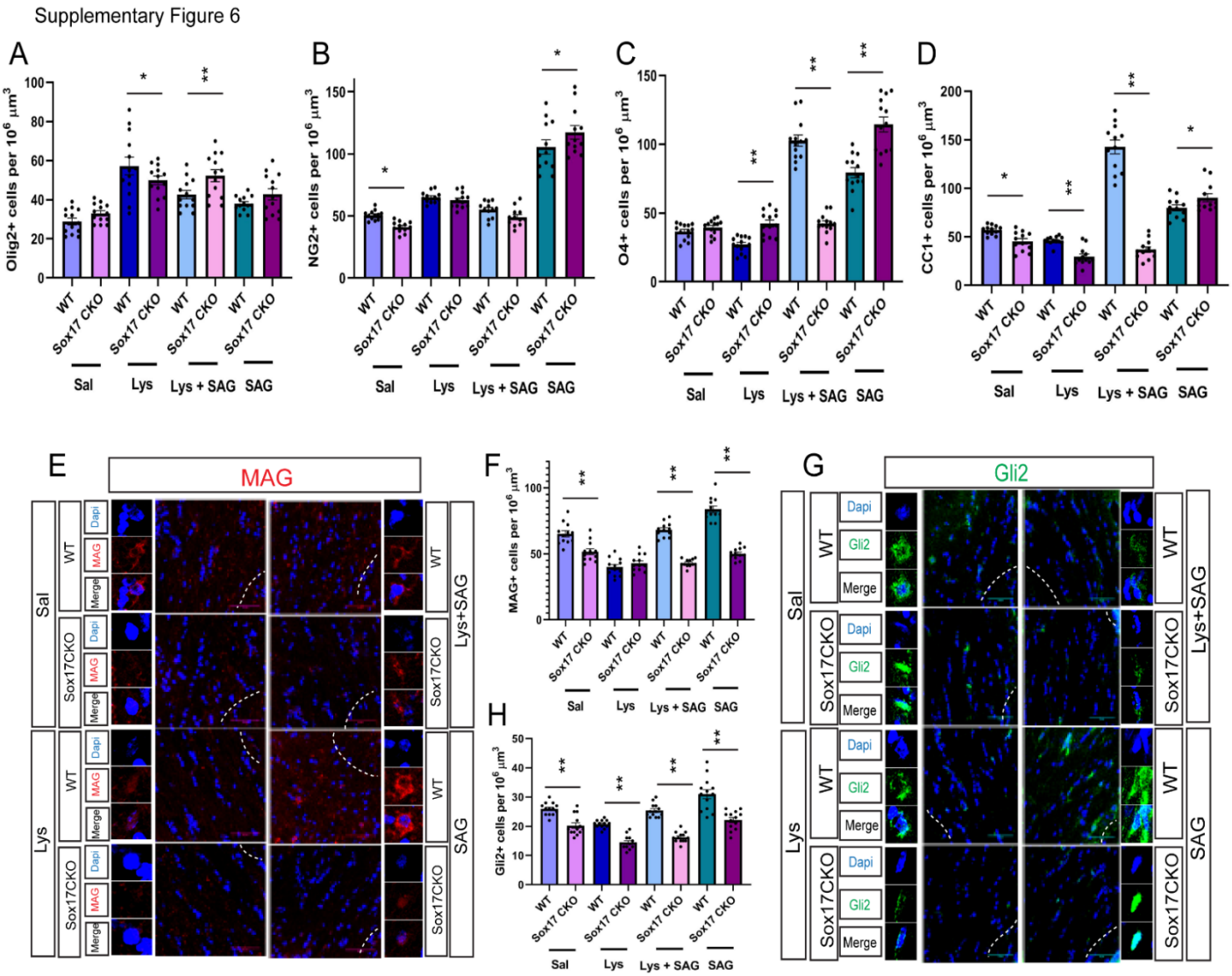


**Supplementary Figure 6. Smoothened activation with 5 uM SAG fails to restore oligodendrocytes in Sox17CKO lesions at 7 DPL. Related to Figure 7.** (A) Quantitative analysis of Olig2+ cells in intact tissue and demyelinating lesions treated with SAG at 7 DPL. (B) Quantitative analysis of NG2+ progenitor cells intact tissue and demyelinating lesions treated with SAG at 7 DPL. (C) Quantitative analysis of O4+ premyelinating oligodendrocyte cells in intact tissue and demyelinating lesions treated with SAG at 7 DPL. (D) Quantitative analysis of CC1+ oligodendrocyte cells in intact tissue and demyelinating lesions treated with SAG at 7 DPL. (E) Confocal microscope images showing MAG-expressing oligodendrocytes (red) in lesions of WT and Sox17CKO WM. Dashed lines delineate WM regions adjacent to injection site. (F) Quantitative analysis of MAG+ myelinating oligodendrocyte cells in intact tissue and demyelinating lesions treated with SAG at 7 DPL. (G) Confocal microscope images showing the effect of SAG administration on Gli2 (green) cells in WT and Sox17CKO WM at 7 DPL. All scale bars = 50 um. (H) Quantitative analysis of Gli2+ cells after SAG administration in intact (Sal) and lesioned (Lys) WM of WT and Sox17CKO mice. Cell density values are mean and SEM obtained from 3 independent litters. Statistical comparisons are provided in Supplementary Tables S1-3. **P*<0.05, ***P*<0.001, Two way ANOVA.

Supplementary Figure 7

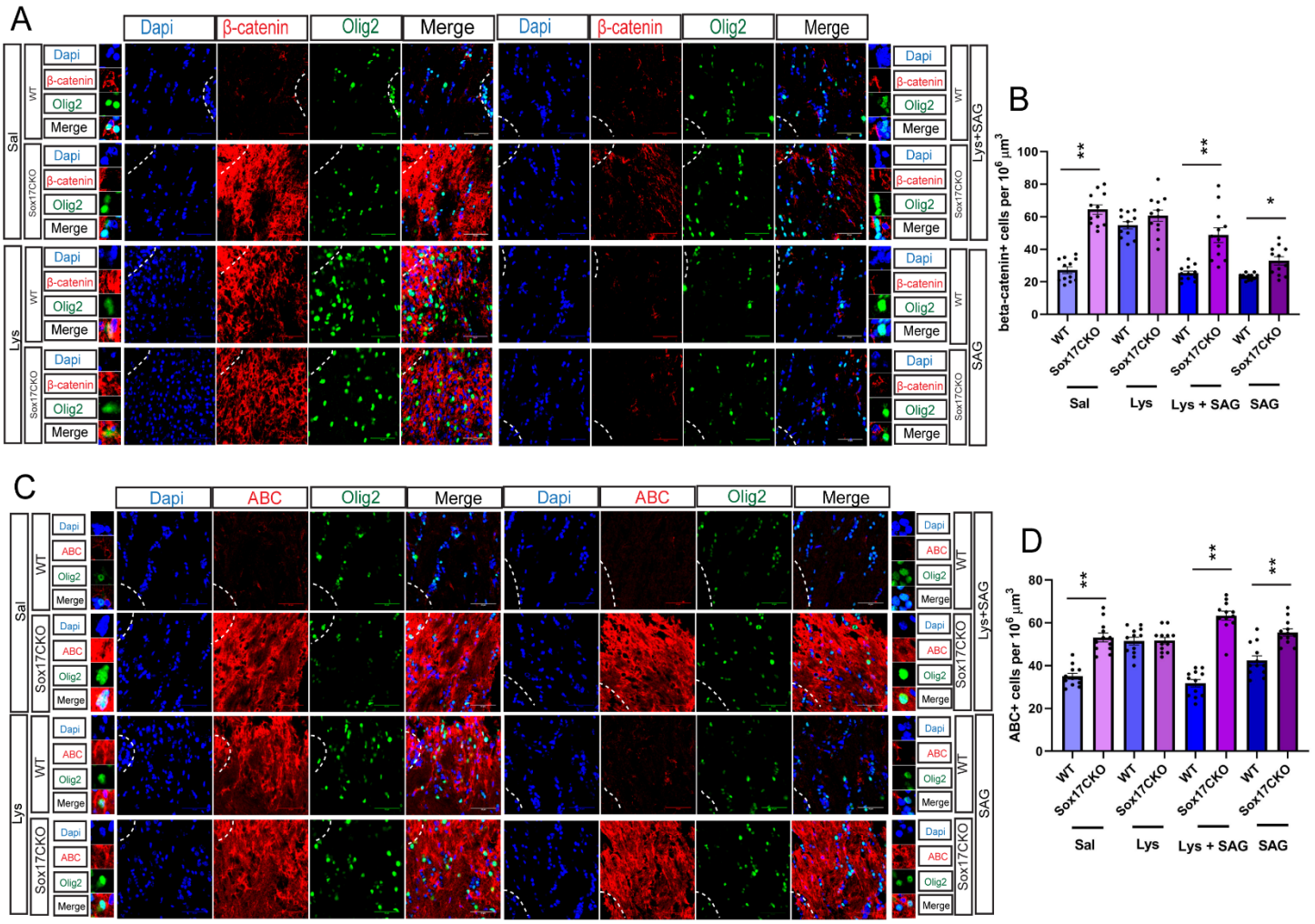


**Supplementary Figure 7. Smoothened activation with 5 uM SAG suppresses beta-catenin in Sox17CKO. Related to Figure 7.** (A) Confocal images showing changes in beta-catenin(red) in Olig2(green)-expressing cells after stereotaxic SAG injection in intact (Sal; SAG) and demyelinating (Lys; Lys+SAG) WM. Scale bar = 50 um. Dashed lines delineate WM regions adjacent to injection site. (B) Quantitative analysis of total beta-catenin+ cells after SAG administration in intact (Sal) and lesioned (Lys) WM of WT and Sox17CKO mice. (C) Confocal images showing changes in ABC (red), Olig2(green)-expressing cells after stereotaxic SAG injection in intact (Sal) and demyelinating (Lys) WM. Scale bars = 50 um.(D) Quantitative analysis of ABC+ cells after SAG administration in intact (Sal) and lesioned (Lys) WM of WT and Sox17CKO mice. Cell density values are mean and SEM obtained from 3 independent experiments. Statistical comparisons are provided in Supplementary Tables S1-S3. **P*<0.05, ***P*<0.001, Two way ANOVA.

**Supplementary Tables**

**Supplementary Table S1 Effect of SAG on changes in cellular response to demyelination in WT WM lesions. Related to Figure 7.**

| | WT | WT | WT | WT | WT | WT |
|---|---|---|---|---|---|---|
| Conditions | Lys/Sal | Lys + SAG/Sal | SAG/Sal | Lys +SAG/Lys | SAG/Lys | SAG/Lys+SAG |
| Olig2 | < 0.001 | 0.001 | 0.031 | < 0.001 | < 0.001 | 0.182 |
| NG2 | 0.006 | 0.317 | < 0.001 | 0.06 | < 0.001 | < 0.001 |
| O4 | 0.034 | < 0.001 | < 0.001 | < 0.001 | < 0.001 | < 0.001 |
| CC1 | 0.037 | < 0.001 | < 0.001 | < 0.001 | < 0.001 | < 0.001 |
| MAG | < 0.001 | 0.252 | < 0.001 | < 0.001 | < 0.001 | < 0.001 |
| Gli2 | <0.001 | 0.846 | <0.001 | <0.001 | <0.001 | <0.001 |
| β-catenin | <0.001 | 0.63 | 0.663 | 0.001 | <0.001 | 0.827 |
| ABC | <0.001 | 0.21 | 0.01 | <0.001 | 0.002 | <0.001 |
| Ki67 | <0.001 | <0.001 | 0.01 | <0.001 | <0.001 | 0.055 |
| Olig2/ABC | <0.001 | 0.673 | 0.644 | <0.001 | <0.001 | 0.823 |
| Olig2/β-catenin | <0.001 | 0.911 | 0.828 | <0.001 | <0.001 | 0.702 |

Significance (*P*) values for pairwise comparisons between conditions, using two way ANOVA.
Red: significantly increased; Blue: significantly decreased; Black: no significant change

**Supplementary Table S2 Effect of SAG on changes in cellular response to demyelination in Sox17CKO WM lesions. Related to Figure 7.**

| | Sox17CKO | Sox17CKO | Sox17CKO | Sox17CKO | Sox17CKO | Sox17CKO |
|---|---|---|---|---|---|---|
| Conditions | Lys/Sal | Lys + SAG/Sal | SAG/Sal | Lys +SAG/Lys | SAG/Lys | SAG/Lys+SAG |
| Olig2 | < 0.001 | < 0.001 | 0.025 | 0.341 | 0.173 | 0.027 |
| NG2 | <0.001 | 0.077 | < 0.001 | 0.007 | < 0.001 | < 0.001 |
| O4 | 0.845 | 0.865 | < 0.001 | 0.797 | < 0.001 | < 0.001 |
| CC1 | 0.008 | 0.19 | < 0.001 | 0.16 | < 0.001 | < 0.001 |
| MAG | 0.009 | 0.01 | 0.821 | 0.926 | < 0.032 | < 0.031 |
| Gli2 | <0.001 | 0.006 | 0.22 | 0.32 | <0.001 | <0.001 |
| β-catenin | 0.325 | <0.001 | <0.001 | 0.005 | <0.001 | <0.001 |
| ABC | 0.584 | <0.001 | 0.578 | <0.001 | 0.364 | 0.012 |
| Ki67 | <0.001 | <0.001 | 0.067 | <0.001 | <0.001 | <0.001 |
| Olig2/ABC | <0.001 | 0.013 | <0.001 | <0.001 | <0.001 | 0.018 |
| Olig2/β-catenin | <0.001 | <0.001 | <0.001 | <0.001 | <0.001 | 0.702 |

Significance *(P)* values for pairwise comparisons between conditions, using two way ANOVA.
Red: significantly increased; Blue: significantly decreased; Black: no significant change

**Supplementary Table S3. Effect of Sox17 ablation on cellular responses to SAG in WM lesions. Related to Figure 7.**

| Comparison | SOX17CKO/WT | SOX17CKO/WT | SOX17CKO/WT | SOX17CKO/WT |
|---|---|---|---|---|
| Condition | Sal | Lys | Lys+SAG | SAG |
| Olig2 | 0.267 | 0.014 | 0.007 | 0.148 |
| NG2 | 0.037 | 0.603 | 0.183 | 0.01 |
| O4 | 0.497 | <0.001 | < 0.001 | 0.001 |
| CC1 | 0.025 | 0.002 | < 0.001 | 0.045 |
| MAG | < 0.001 | 0.279 | < 0.001 | <0.001 |
| Gli2 | <0.001 | <0.001 | <0.001 | <0.001 |
| β-catenin | <0.001 | 0.122 | <0.001 | 0.012 |
| ABC | <0.001 | 0.923 | <0.001 | <0.001 |
| Ki67 | 0.001 | <0.001 | <0.001 | 0.02 |
| Olig2/ABC | <0.001 | 0.269 | <0.001 | 0.311 |
| Olig2/β-catenin | <0.001 | <0.001 | 0.898 | 0.898 |

Significance (*P*) values for pairwise comparisons between Sox17CKO vs WT, using two way ANOVA.
Red: significantly increased; Blue: significantly decreased; Black: no significant change

**Supplementary Table S4. Primary antibodies. Related to Transparent Methods.**

| Primary Antibody | Catalog No. | Clone | Isotype | Host | Dilution for Immunohistology | Dilution for Western blot | Vendor |
|---|---|---|---|---|---|---|---|
| Beta-catenin | 610153 | | | Mouse | 1:500 | 1:500 | BD Transduction Laboratories |
| Active-β-Catenin (ABC) | 05-665 | | Ig | Mouse | 1:500 | 1:500 | Millipore |
| p-beta-catenin (Ser33/37/Thr41) | 9561 | | Ig | Rabbit | 1:300 | N/A | Cell Signaling Technology |
| MBP | SMI-99 | | IgG2b | Mouse | 1:1000 | 1:2000 | Covance Inc |
| Gli2 | ab7195 | | IgG | Rabbit | 1:500 | 1:200 | Abcam |
| BrdU | ab6326 | | IgG2a | Rat | 1:300 | | Abcam |
| MAG | sc-15324 | H-300 | | Rabbit | | 1:500 | Santa Cruz |
| SHH | Sc-9024 | | | Rabbit | 1:200 | | Abcam |
| Human biotinylated SOX17 | BAF1924 | Asp177-Val414 | IgG | Goat | 1:100 | 1:50 | R&D Systems |
| NG2 | Ab5320 | | Ig | Rabbit | 1;100 | N.A. | Millipore |
| O4 | MAB1326 | O4 | IgM | Mouse | 1:200 | N.A. | R&D Systems |
| Cleaved Caspase-3 | 9664S | | IgG | Rabbit | 1:50 | N.A. | Cell Signaling Technology |
| Olig2 | AB9610 | | Ig | Rabbit | 1:500 | N.A. | Millipore |
| Olig2 | MABN50 | 211F1.1 | IgG | Mouse | 1:250 | N.A. | Millipore |
| CC1 | OP80 | CC1 | IgG2b | Mouse | 1:500 | N.A. | Calbiochem |
| Smoothened | ab72130 | | IgG | Rabbit | 1:250 | N.A. | Abcam |
| Oct4 | Ab3209 | | IgG | Rabbit | 1:200 | 1:100 | EMD Millipore |
| LacZ | BGL-1040 | | | Chicken | 1:3000 | N.A. | AVES |
| Ki67 | M7240 | MIB-1 | IgG1κ | Mouse | 1:100 | N.A. | DAKO |
| Iba1 | 019-19741 | | | Rabbit | 1:500 | N.A. | Wako |
| Sox2 | ab97959 | | | Rabbit | 1:200 | N.A. | Abcam |

**Supplementary Table S5. Secondary conjugated antibodies. Related to Transparent Methods.**

| Secondary Antibody | Catalog No. | Isotype | Host | Anti- | Dilution for Immunohistochemistry | Dilution for Western blot | Vendor |
|---|---|---|---|---|---|---|---|
| IRDye 800CW | 926-32210 | IgG (H + L) | Goat | Mouse | N.A. | 1:2000 | Odyssey(Li-CoR) |
| IRDye 800CW | 926-32213 | IgG (H + L) | Donkey | Rabbit | N.A. | 1:2000 | Odyssey(Li-CoR) |
| IRDye 680LT | 926-68020 | IgG (H + L) | Goat | Mouse | N.A. | 1:2000 | Odyssey(Li-CoR) |
| IRDye 680LT | 926-68023 | IgG (H + L) | Donkey | Rabbit | N.A. | 1:2000 | Odyssey(Li-CoR) |
| IRDye 680LT | 926-68031 | Conjugate Streptavidin | | Biotinylated antibody | N.A. | 1:1000 | Odyssey(Li-CoR) |
| Rhodamine | 111-295-144 | IgG (H + L) | Goat | Rabbit | 1:250 | N.A. | Jackson Immunoresearch |
| Cy5 | 111-605-144 | IgG (H + L) | Goat | Rabbit | 1:200 | N.A. | Jackson Immunoresearch |
| Alexa Fluor® 647 | A31573 | Ig(H+L) | Donkey | Rabbit | 1:300 | N.A. | Invitrogen |
| Alexa Fluor® 647 | A21237 | Ig(H+L) | Goat | Mouse | 1:300 | N.A. | Invitrogen |
| Alexa Fluor® 546 | A10036 | Ig(H+L) | Donkey | Mouse | 1:500 | N.A. | Invitrogen |
| Alexa Fluor® 546 | A11071 | IgG (H+L | Goat | Rabbit | 1:500 | N.A. | Invitrogen |
| Alexa Fluor® 594 | S32356 | Conjugate Streptavidin | | Biotinylated antibody | 1:500 | N.A. | Invitrogen |
| Alexa Fluor® 647 | S32357 | Conjugate Streptavidin | | Biotinylated antibody | 1:300 | N.A. | Invitrogen |

## TRANSPARENT METHODS

## MATERIALS

### Animals

CNPSox17ZsGreen transgenic mice (abbreviated CNPSox17) were maintained as previously described (Ming et al., 2013). Gli2f/f and Smof/f mouse strains were obtained from Jackson laboratory (Cat #007922, #004526) or were a kind gift from Dr Alex Joyner (Sloan Kettering Institute, NY). All mouse strains, including WT (C57BL/6, cat #003548, Jackson Laboratory), PDGFRCreERT2 (Kang et al., 2010), BATGAL (Maretto et al., 2003) (Cat #005317, Jackson Laboratory), were maintained in the Research animal facility of the Children's National Health System according to the Institutional Animal Care and Use Committee and the National Institutes of Health guidelines. In order to conditionally ablate Gli2 in OPCs, we crossed Gli2f/f mice with PDGFR$\alpha$CreERT2 transgenic mice (abbreviated as PCre), which express the tamoxifen-inducible form of Cre in OPCs. To ablate Gli2 from OPCs of CNPSox17 mice, the following breeding strategy was used: PCre;Gli2f/f were crossed with heterozygous CNPSox17 to obtain CNPSox17+/-; PCre;Gli2f/+, which were subsequently bred with PCre+Gli2f/+ or Gli2f/+ mice to obtain CNPSox17+/-;PCre+;Gli2f/f mice. CNPSox17+/-;PCre+;Smof/f mice were obtained using a similar breeding strategy. Genotyping procedures for Gli2f/f and Smof/f were performed using the protocols and primer sequences provided by the Jackson Laboratory. Cre and Sox17f/f genotyping primer sequences are as follows: Cre Forward GCG GTC TGG CAG TAA AAA CTA TC; Cre Reverse GTG AAA CAG CAT TGC TGT CAC TT; Sox17 flox Lox1 Forward CAG CCT TCC TAT TTC CCC AAG AGG; Sox17 flox Lox3 Reverse CTG GTC GTC ACT GGC GTA TCC. CNPCre; Sox17f/f mice (Sox17CKO) and PDGFRaCreERT2;Sox17f/f (Sox17PCKO) mice were recently described (Chew et al., 2019). PCR products were resolved on 2% TAE agarose gels.

### Lysolecithin(LPC)-induced demyelination, BrdU and drug injections

Focal demyelination using lysolecithin (LPC) was performed in adult (P40-P60) WT mice after deep ketamine/xylazine anesthesia (10mg/g body weight). Mice were placed in a stereotaxic frame (Stoerling) and injected into the cingulate WM with 2 µl of 1% LPC solution using Hamilton micropipettes (Stoerling). The

contralateral side received an equivalent volume of 0.9% NaCl as control. Injection time lasted 5 min to reduce reflux along the needle track. Stereotaxic coordinates for subcortical cingulate WM were : from bregma: 0.26 mm caudal, 1.0 mm lateral, and 2.5 mm ventral. The day of injection was designated as day 0. Mice were processed for immunocytochemistry at 3 or 7 days after LPC or control NaCl injections. Signaling inhibitors were from EMD Calbiochem (Burlington, MA). CCT036477 (10uM, Cat 68-167-45MG), cyclopamine(5uM, Cat 239804), Gant-61(5uM,Cat 373403) or SAG(5uM, Cat 566660) in DMSO were either injected alone or together with lysolecithin into the CC. Control injections consisted of DMSO diluted in 0.9% NaCl. Bromodeoxyuridine (BrdU) was injected i.p. at 50 mg/kg. Tamoxifen was injected i.p. at 2 days before lysolecithin demyelination, twice a day, at 75 mg/kg. Mice were generally sacrificed at 3DPL unless otherwise stated.

**Immunocytochemistry and histological analyses**

Immunocytochemistry was performed on floating sections using antibodies listed in Tables S4 and Table S5. The techniques were previously described (Aguirre et al., 2005). Briefly, sections were incubated overnight at 4°C in primary antibodies diluted in 0.1 M PBS (pH7.4), containing 0.1% Triton and 5% normal goat serum. After washing with PBS, sections were incubated with secondary antibodies for 1 hour at room temperature and then mounted. Z-stacks of 1µm-thick optical sections through the entire thickness of slice were captured using a confocal microscopy - MRC1024, BioRad Laboratories; Zeiss LSM 510, or Leica TCS SP8 laser scanning confocal microscopes, acquired with Zen or LasX under 40 or 64X oil objectives respectively, using a Z step of 1 um, and collapsed along z-axis before cell counting. Demyelinated lesions were verified by decreased CC1 and MBP immunoreactivity. For saline-injected tissue, the injection site was localized by its needle track and the injection site on the dorsal surface of the brain. Measurements were taken from 7-12 tissue sections obtained from 3-4 mice in each group. The results are presented as a mean ± SEM, and Student's unpaired *t*-test was performed to test the hypothesis of means' equality.

**Reporter Assays**

8XGliBSLuciferase reporter plasmid was a kind gift from Dr Pao-Tien Chuang (UCSF), TOPFLASH and FOPFLASH purchased from Upstate Cell Signaling Solutions, pCS2-MT GLI2 deltaN (Gli2dN) and pCS2-MT

Gli2FL were obtained from Addgene, and mouse Gli1 TrueClone was obtained from Origene (Rockville, MD). For transient transfection, human oligodendroglioma (HOG) and HEK cells were plated in 10% FBS/DMEM at 3x $10^4$ per well in 12-well plates 24h prior to transfection in DME-N1 medium. Cells received 0.4 ug of 8xGLIBS-Luc, Axin2-luciferase reporter or TOPFLASH (Millipore, Billerica, MA) reporter plasmid, 0.4 ug of Gli2 delta N, Gli3 FL or GLI 1 expression vectors with 0.4ug CMVTnT vector and 0.02 ug of SV40-beta-galactosidase in 500ul of N1 with 2.4 ul of Lipofectamine 2000. Combinations of expression vectors included 0.4ug bCatS37A and 0.4ug GLI plasmids. After overnight incubation with the DNA-lipofectAMINE complexes, the medium was replaced with 10% FBS/DEMEM, and harvested 48h after the start of transfection. Transfected cells were collected in 150-200 ul of reporter lysis buffer (Promega) and, after three freeze-thaw cycles and clearing, 50ul of lysate was assayed for luciferase activity on a Turner 20/20n luminometer (Turner Biosystems, Sunnyvale, CA). Luciferase activity expressed as relative light units was normalized with total protein content by BCA assay (Pierce, Rockford, IL) or beta-galactosidase activity. Following measurement of luciferase activities, results were normalized by protein or beta-galactosidase and are reported as a ratio of TOPFLASH/FOPFLASH for any given treatment.

**Western Blot and Immunoprecipitation**

White matter tissue was dissected and homogenized in RIPA lysis buffer with proteinase inhibitors (Santa Cruz Biotech, Inc, Sc 24948). For Western blotting, following quantification with BCA kit (Pierce Thermofisher) protein extracts were mixed with SDS loading buffer (Pierce Thermofisher) and boiled for 5 min prior to loading onto 4-20 % gradient gels (GeneMate, E4326-420, 20 µg of protein per each lane). Extracted proteins were resolved on 4-20 % Tris-Glycine gels followed by 2 hr or overnight transfer onto membranes (Immobilon®-F for Odyssey system). After blocking in Odyssey blocking buffer, blots were incubated with primary antibodies overnight at 4C, and visualized with secondary antibodies using the Li-CoR infrared Imaging system. Alternatively, proteins transferred to Immobilon®-P were visualized with HRP-conjugated antibodies followed by chemiluminescence detection with ECL substrate (Amersham, RPN2132 or Perkin Elmer Western Lightning Plus-ECL, NEL103001EA). The antibodies used for Western blotting are listed in Table S4 and Table S5.

**Electron Microscopy**

Mice were prepared for electron microscopic analysis as previously described (Aguirre et al., 2007; Marcus et al., 2006). Following transcardial perfusion with 0.1M Millonig's buffer containing 4% paraformaldehyde and 2.5% glutaraldehyde and brain removal, a coronal brain matrix (Ted Pella, Redding, CA) was used to cut the brain in serial 1 mm slices. Comparable slices for each brain (~0.5mm anterior to bregma were rinsed 3X in 0.1M cacodylate buffer, post fixed in 1% osmium tetroxide (in cacodylate buffer), dehydrated in increasing dilutions of ethanol and embedded in PolyBed resin. Thick (1µm) and thin (70nm) sections were stained with toluidine blue or with a combination of uranyl acetate and lead citrate, respectively. A minimum of 10 electron micrographs within the corpus callosum region were captured at both low (5,000X) and high (20,000X) magnifications per mouse using a JEOL JEM 1230 transmission electron microscope equipped with a Gatan 4K X 4K Ultrascan digital camera.

Low magnification images were used to qualitatively assess the overall extent of myelination; high magnification images were used for quantitative analyses. The percent myelinated and unmyelinated axons was determined and G ratio analysis was conducted. Any axon with a single wrap of an oligodendrocyte process was classified as "myelinated"; G ratio analyses were limited to only myelinated axons and were calculated by dividing the average axon diameter determined by measuring the longest and shortest diameter by the average axon diameter plus the width of the thickest and narrowest span of the myelin sheath in cross section. For myelin thickness measurements, regions with expanded myelin due to structural artifact were not used. Analyses were limited to axons with a caliber of >0.3 µm since previous work has shown that CNS axons ≤ 0.3µm are not myelinated (Mason et al., 2001).

**Statistical analysis**

All animal experiments involve at least three animals per group. Significance levels for comparison between groups were determined with unpaired two-tailed Student's *t*-test, one-way or two-way ANOVA with Holm-Sidak post-hoc tests, using Sigmaplot v13 (Systat Software, Inc, CA) or Prism 7 (GraphPad Software, San Diego, CA). Quantification data are plotted as mean ± S.E.M. N values represent independent experiments.

Significance levels used were generally * for $P<0.05$, ** for $P< 0.01$ and *** for $P<0.001$, unless otherwise stated. The use of specific statistical tests is indicated in Figure Legends, together with sample size information.

**REFERENCES**


Aguirre, A., Rizvi, T.A., Ratner, N., and Gallo, V. (2005). Overexpression of the epidermal growth factor receptor confers migratory properties to nonmigratory postnatal neural progenitors. J Neurosci *25*, 11092-11106.

Aguirre, A.A., Dupree, J.L., Mangin, J.M., and Gallo, V. (2007). A functional role for EGFR signalling in myelination and remyelination. Nat Neurosci *10*, 990-1002.

Kang, S.H., Kukaya, M., Yang, J.K., Rothstein, J.D., and Bergles, D.E. (2010). NG2+ CNS glial progenitors remain committed to the oligodendrocyte lineage in postnatal life and following neurodegeneration. Neuron *68*, 668-681.

Marcus, J., Honigbaum, S., Shroff, S., Honke, K., Rosenbluth, J., and Dupree, J.L. (2006). Sulfatide is essential for the maintenance of CNS myelin and axon structure. GLIA *53*, 372-381.

Maretto, S., Cordenonsi, M., Dupont, S., Braghetta, P., Broccoli, V., A.B., H., Volpin, D., Bressan, G.M., and Piccolo, S. (2003). Mapping Wnt/beta-catenin signaling during mouse development and in colorectal tumors. Proc Natl Acad Sci (USA) *100*, 3299-3304.

Mason, J.L., Langaman, C., Morell, P., Suzuki, K., and Matsushima, G.K. (2001). Episodic demyelination and subsequent remyelination within the murine central nervous system: changes in axonal calibre. Neuropathol Appl Neurobiol *27*, 50-58.